Dickkopf-1 Promotes Angiogenesis by Upregulating VEGF Receptor 2-mediated mTOR/p70S6K Signaling in Hepatocellular Carcinoma

Sang Hyun Seo
Yonsei University College of Medicine
Kyung Joo Cho
Yonsei University College of Medicine
Hye Jung Park
Yonsei University College of Medicine
Hyemi Kim
Yonsei University College of Medicine
Hye Won Lee
Yonsei University College of Medicine
Beom Kyung Kim
Yonsei University College of Medicine
Jun Yong Park
Yonsei University College of Medicine
Do Young Kim
Yonsei University College of Medicine
Sang Hoon Ahn
Yonsei University College of Medicine
Seung Up Kim (KSUKOREA@yuhs.ac)
Yonsei University College of Medicine

Research

Keywords: Dickkopf-1, Vascular endothelial growth factor receptor 2, Hepatocellular carcinoma, Angiogenesis, Epithelial-mesenchymal transition, mammalian target of rapamycin, p70 S6 kinase

Posted Date: December 15th, 2020

DOI: https://doi.org/10.21203/rs.3.rs-125332/v1

Abstract

Background: The expression of Dickkopf-1 (DKK1), a negative regulator of the Wnt/β-catenin signaling pathway, is upregulated in hepatocellular carcinoma (HCC). Here, we investigated the tumorigenic and angiogenic potential of DKK1 in HCC.

Methods: Stable cell lines were established using the clustered regularly interspaced short palindromic repeats (CRISPR)-associated nuclease 9 (CRISPR/Cas9)-based DKK1 knock-out system in Hep3B cells and the tetracycline-based DKK1 inducible system in Huh7 cells. Multicellular tumor spheroids (MCTSs) were cultured using Hep3B stable cells. We also employed xenografts generated using Hep3B stable cells and transgenic mouse models established using hydrodynamic tail vein injection.

Results: The angiogenic potential increased in HUVECs treated with CM from Huh7 stable cells with high DKK1 expression and Hep3B wild-type cells. There was an increase in the phosphorylation of vascular endothelial growth factor receptor 2 (VEGFR2) and p70 S6 kinase (p70S6K), which are downstream proteins of VEGFR2-mediated mTOR/p70S6K signaling. MCTSs generated using Hep3B wild-type cells promoted compact spheroid formation and raised expression of CD31 and epithelial-mesenchymal transition (EMT) markers, compared to the controls (all P<0.01). Xenograft tumors generated using Hep3B cells with DKK1 knock-out (n=10) exhibited slower growth than, the controls (n=10) and the expression of Ki-67, VEGFR2, CD31 and EMT markers decreased (all P<0.05). In addition, forced DKK1 expression with HRAS in transgenic mouse livers (n=5) resulted in the formation of more tumors and increased expression of Ki-67, VEGFR2, CD31, and fibronectin, compared to the controls (n=5) (all P<0.05).

Conclusions: Our findings indicate that DKK1 facilitates angiogenesis and tumorigenesis by upregulating VEGFR2-mediated mTOR/p70S6K signaling in HCC.

Background

Hepatocellular carcinoma (HCC), the primary cancer of the liver, is derived from hepatocytes and occurs in more than approximately 80% of cases of liver cancer (1). HCC is a hypervascular tumor in which angiogenesis plays an important role in development, invasion and metastasis (2). Tumor growth relies on angiogenesis, the formation of new blood vessels from pre-existing vasculature, to receive an adequate supply of oxygen and nutrients into the tumors (3, 4). Accordingly, anti-HCC agents, such as sorafenib and lenvatinib, which target vascular endothelial growth factor (VEGF), fibroblast growth factor (FGF), and platelet-derived growth factor (PDGF) receptors have shown survival benefits in HCC treatment (5).

Pro-angiogenic factors such as VEGF, FGF and PDGF are known to activate tyrosine kinases and subsequent downstream intracellular signaling through mitogen-activated protein kinase (6). Both VEGF and VEGF receptors (VEGFRs), the most prominent and widely researched regulators of angiogenesis, are critical for HCC growth and development (7). The binding of VEGF to VEGFR leads to endothelial

proliferation and migration as well as formation and branching of new tumor blood vessels (8). In addition, VEGFR1 activation upregulates the expression of epithelial-mesenchymal transition (EMT)-associated factors, such as Snail, Twist and Slug in HCC (9).

Dickkopf-1 (DKK1), which binds to the low-density lipoprotein receptor-related protein-5/6 Wnt co-receptor, is a secreted protein that functions as a negative regulator of Wnt signaling (10–15). Wnt signaling regulates diverse cellular and biological processes such as proliferation, survival, migration and liver development (16–18). In addition, the DKK protein family has been found to regulate angiogenesis, and it has been reported that the Wnt signaling pathway and DKK1 modulate tumorigenesis during vasculogenesis and angiogenesis (19).

Several studies have reported that DKK1 expression is upregulated in HCC cell lines (20–22) and the tumor tissues and serum samples of patients with HCC (20, 23, 24). Ectopic DKK1 expression promotes HCC cell migration and invasion through β-catenin/matrix metalloproteinase 7 (MMP7) signaling (25). Moreover, the downregulation of DKK1 expression using siRNA has been shown to inhibit invasion and metastasis in HCCLM3 cells. In contrast, DKK1 overexpression in the HepG2 cell line has been shown to significantly promote its migration and invasiveness (26). These results indicate that DKK1 regulation can be a promising target for angiogenesis in HCC.

In a previous study, we showed that DKK1 induces angiogenesis by regulating VEGF receptor 2 (VEGFR2) (27), but the correlation between DKK1 and angiogenesis in HCC remains poorly understood. In the present study, we investigated the angiogenic and tumorigenic role of DKK1 in HCC using diverse models of regulated DKK1 expression and found that DKK1 promotes angiogenesis by upregulating VEGFR2-mediated mammalian target of rapamycin (mTOR)/p70 S6 kinase (p70S6K) signaling in HCC.

Methods

Cell lines

Huh7 (Korean Cell Line Bank, Seoul, Korea), GP2-293 (Clontech, California, USA), Hep3B, LX2 [Dr. Seo (28)] and WI38 cells were cultured at 37°C with 5% CO_2 in Dulbecco's Modified Eagle's Medium (Gibco, Carlsbad, CA, USA), Modified Eagle's Medium (Gibco) or RPMI-1640 (Gibco) supplemented with 10% fetal bovine serum (Gibco) and 1x penicillin-streptomycin (Welgene, Daegu, Korea). Human umbilical vein endothelial cells (HUVECs) were cultured in Medium 200 (Gibco) supplemented with low serum growth supplement (Gibco) at 37°C with 5% CO_2.

Generation of stable cell lines

Stable cell lines were generated using the clustered regularly interspaced short palindromic repeats (CRISPR)-associated nuclease 9 (CRISPR/Cas9)-based DKK1 knockout system in Hep3B cells and the tetracycline-based DKK1 inducible system in Huh7 cells. Alt® CRISPR-Cas9 system, CRISPR RNA (crRNA):

Guide RNA (gRNA) targeting the human DKK1 locus along with transactivating crRNA (tracrRNA), were obtained from Integrated DNA Technologies (San Diego, CA, USA) for Hep3B stable cell line. crRNA was used to select target region within the first exon of the human DKK1 gene. Tracr and crRNA were combined according to the manufacturer's protocol and then crRNA: tracrRNA duplexes were with Cas9 protein. Subsequently, the Alt® CRISPR-Cas9 system was transfected into Hep3B cells using Lipofectamine™ RNAiMAX (Thermo Fisher Scientific, Waltham, MA, USA). Off-target effects in the two selected stable cell line clones were identified using by whole genome sequencing (Promega, Madison, WA, USA).

GP2-293 was transfected to make regulator (Retro-X Tet-On Advanced Inducible Expression System and pVSV-G) and response (pRetroX-tight Pur-DKK1/pVSV-G or pRetroX-tight Pur-Mock/pVSV-G) plasmid (Clontech, California, USA) using CalPhos Mammalian Transfection Kit (Clontech). The regulator plasmid was added to the culture medium of Huh7 cells. Transfected Huh7 cells were selected by on the basis of resistance to the antibiotic, G418 (Takara Bio Inc, Seoul, Korea), followed by the addition of the response plasmid to the culture medium of the selected Huh7 cells. Twenty-four hours after infection, the cells were subjected to puromycin (Takara Bio Inc) selection.

Assessment of DKK1 using ELISA

The concentration of DKK1 in HCC cell lines was measured using enzyme-linked immunosorbent assay (ELISA) kits (R&D systems, Minneapolis, MN, USA), according to the manufacturer's instructions. Subsequently, all the groups of supernatants were collected and DKK1 levels were assayed in them.

Cell invasion, tube formation and wound healing assay

The invasiveness of HUVECs was assessed using a transwell chamber (Corning Costar, Cambridge, MA, USA). Next, 3x 10^4 HUVECs/well were treated with VEGF or recombinant (rDKK1) in each transwell chamber. Following incubation for 24 h, the invading cells were stained with hematoxylin and eosin (H&E). The total number of invaded cells on the lower side of the filter was determined using a light microscope (Olympus, Tokyo, Japan) at 40x magnification.

Tube formation by HUVECs was measured using Matrigel® (Corning). A 48 well plate (BD Falcon®, Bedford, MA, USA) was coated with 150 µL Matrigel® and seeded with HUVECs (3x 10^4/well), followed by the addition of conditioned medium (CM) from Hep3B and Huh7 stable cell lines. The plates were incubated for 4 h, following which tube formation was observed under a light microscope.

Wound healing assays were performed by creating identical wound areas into the cell monolayer using culture-inserts (Ibidi GmbH, Munich, Germany). A 24 well plate was coated with 2% gelatin (BD Biosciences) and seeded with HUVECs (2x 10^4/well) on each side of the culture-insert. After attachment,

the cells were treated with CM from the HCC stable cell line, followed by detachment of the culture-insert. The wound images were captured at 0 and 6 h using a light microscope.

mRNA isolation and RT-PCR

For PCR, total RNA was extracted using TRIzol™ reagent (Invitrogen, California, USA) and synthesis of first strand cDNA (Superscript™ III First-Strand Synthesis System, Invitrogen) was performed according to the manufacturer's recommended protocols. A PCR master mix (Power SYBR™ Green PCR Master Mix; Applied Biosystems, Warrington, UK) was used for quantitative PCR performed on the StepOnePlus™ PCR System (Applied Biosystems).

Western blot analysis

Cells and tissues were washed and lysed with RIPA buffer containing a protease inhibitor cocktail (Thermo Fisher Scientific) and a phosphatase inhibitor cocktail (GenDEPOT, Katy, TX, USA). Cell and tumor lysates were cleared using centrifugation, separated using SDS-PAGE and transferred to polyvinylidene fluoride membranes. The membranes were incubated with antibodies against DKK1 (R&D Systems), VEGFR2, p-VEGFR2, mTOR, phospho-P70S6 kinase (p-p70S6K), GAPDH, phosphoinositide 3-kinase (PI3K) and p-Akt (Cell Signaling Technology, Danvers, MA, USA) at the recommended concentrations. The blots were developed using the enhanced chemiluminescence technique (PerkinElmer, Waltham, MA, USA) according to the manufacturer's instructions.

Spheroid fabrication

Hep3B-only or hybrid spheroids were fabricated in a low attachment multiple well plate (Corning). To model tumor complexity and heterogeneity, we formed multicellular tumor spheroids (MCTSs) with Hep3B stable cell lines and stromal cells, such as HUVECs (human endothelial cells), LX2 (human hepatic stellate cells) and WI38 (human fibroblasts) and counted them prior to mixing them in the desired ratio. A 200 μL cell mixture of these four cell types was prepared in the following ratio: Hep3B stable cells: HUVECs: LX2: WI38=4: 2: 1: 1. This mixture was subsequently pipetted onto the plate. Images of MCTS were acquired using a microscope (Olympus) and imported into ImageJ software. The average radius (r) was then calculated using ImageJ software and used to obtain the volume value (V) with the following formula: $V=4/3\pi r^3$.

Animals

All experiments involving live mice were performed according to the Guidelines and Regulations for the Care and Use of Laboratory Animals in AAALAC-accredited facilities, and were approved by the Animal

Policy and Welfare Committee of the Yonsei University College of Medicine (Permit number: 2018–0088). We purchased 4–5-week-old C57BL/6 male mice from Orientbio (Seongnam, Korea), while 4-week-old BALB/c nude male mice were purchased from Central Lab. Animal Inc. (Seoul, Korea).

Xenograft mouse model

The Hep3B stable cell line (5x 10^6 or 7x 10^6 cells) in HBSS was mixed with Matrigel® [2:1] (Corning) and then inoculated subcutaneously into the left and right flanks of each BALB/c nude mouse. Tumors were monitored once a week and the tumor volume was calculated with the help of Vernier calipers. The volumes of the tumors were calculated using a standard formula (length x $width^2$ x 0.5) and growth curves were drawn. Nine weeks later, animals in all the groups were sacrificed, following which their tumors were harvested and fixed in 10% formalin.

Histology analysis

The specimens embedded in paraffin blocks were sectioned into 4-μm slices. Specimens for histological analysis were processed using conventional H&E staining for the visualization of general tissue morphology. Stained specimens were inspected using a microscope (Olympus).

Immunohistochemistry and immunofluorescence

Paraffin sections were deparaffinized in xylene and rehydrated through a gradual decrease in ethanol concentration. The antigen epitopes were then unmasked using sodium citrate buffer (pH=6.0). Subsequently, the sections were incubated overnight at 4°C using the following primary antibodies: anti-Ki-67 (Cell Signaling Technology), anti- anti-cluster of differentiation 31 (CD31) (Invitrogen) and anti-HRAS (Santa Cruz Biotechnology, California, USA). After primary incubation, the sections were incubated with the appropriate biotinylated secondary antibodies followed by treatment with freshly prepared 3,3'-diaminobenzidine substrates (Vector Laboratories, Burlingame, CA, USA). Sections were lightly counter-stained with hematoxylin and mounted. For immunofluorescence (IF), the sections were probed with anti-DKK1 (R&D systems), CD31 (Invitrogen), anti-VEGFR2, anti-vimentin, anti-fibronectin and anti-E-cadherin antibodies (Cell Signaling Technology). Next, after washing with phosphate-buffered saline, the sections were incubated with secondary antibodies, stained with 4',6-diamidino-2-phenylindole and then embedded Fluoromount-G™ (Invitrogen). Fluorescence images were obtained using a Zeiss LSM 700 confocal microscope (Carl Zeiss, Oberkochen, Germany).

Hydrodynamic tail-vein injection

The plasmids pT2/HRAS^{G12V}, pT2/shp53, and PT2/C-Luc/PGK-SB13 were prepared using endotoxin-free EndoFree® Plasmid Maxi Kit (Qiagen, Hilden, Germany). DNA mixtures of transposons (pT2 plasmids) and transposase-encoding vector (pPGKSB13) were suspended in Lactated Ringer's solution and subsequently injected into the lateral tail veins of 5- to 6-week old male mice (0.1 mL/g body weight) in less than 7 s. The livers were harvested 5 weeks following the hydrodynamic transfection, unless specified otherwise.

Statistical analysis

Statistical analyses were conducted using an unpaired parametric Student's t-test or Fisher's

exact test, as appropriate. A value of $P<0.05$ was chosen to indicate statistical significance.

Results

Establishment and characterization of stable cell lines

Treatment with rDKK1 resulted in a concentration-dependent enhancement of the invasive potential of HUVECs (Figure 1A). Upon confirmation of the expression of DKK1 in various human HCC cell lines, it was found that the levels of secreted DKK1 were high in Hep3B cells, but low in Huh7, SNU475, and SNU449 cells (Supplementary Figure 1). Accordingly, Huh7 cells with low DKK1 expression and Hep3B cells with high DKK1 expression were selected for the regulation of DKK1 expression. Stable cell lines were established using the CRISPR-Cas9-based DKK1 knockout system in Hep3B cells and the tetracycline-based DKK1 inducible system in Huh7 cells. We used the CRISPR-Cas9 system to select the target region within exon-1 of the human DKK1 gene. Subsequently, several colony cell lines were established by transfection, and it was found that the sizes of the DKK1 exon-1 in colonies 73 (Hep3B CRISPR#73 cells) and 131 (Hep3B CRISPR#131 cells) were smaller than those of the positive control (Hep3B wild-type cells) (Supplementary Figure 2). We also observed that the expression of DKK1 and the protein levels of secreted DKK1 in Hep3B wild type cells were significantly higher than those of Hep3B CRISPR#73 and #131 cells (Figure 1B). However, since the protein level of secreted DKK1 in Hep3B CRISPR#131 cells was higher than those in CRISPR#73 cells ($P<0.001$), Hep3B CRISPR#73 cells were used in the current study (Figure 1C). In addition, protein expression of DKK1 was significantly higher in doxycycline-treated pRetroX-tight Pur-DKK1 transfected Huh7 cells (Huh7 Pur-DKK1 cells) than in Huh7 wild-type cells and doxycycline-untreated Huh7 Pur-DKK1 cells and pRetroX-tight Pur-Mock transfected Huh7 cells (Huh7 Pur-Mock cells) (Figure 1D). In addition, we confirmed that the protein levels of secreted DKK1 were higher in Huh7 Pur-DKK1 cells than in Huh7 Pur-Mock cells, when the Huh7 stable cells were treated with doxycycline for 24 and 48 h (Figure 1E).

DKK1 enhances the angiogenic potential of HUVECs

We investigated whether DKK1 regulates endothelial cell tube formation and migration, which are two important features of angiogenesis (29). Tube formation was enhanced in HUVECs treated with concentrated CM from doxycycline-treated in Huh7 Pur-DKK1 cells, whereas it was not enhanced in HUVECs treated with concentrated CM from Hep3B CRISPR#73 cells, compared to the controls (Figure 2A). In addition, HUVECs treated with CM from doxycycline-treated in Huh7 Pur-DKK1 and Hep3B wild-type displayed higher migration ability than the controls (Figures 2B-C). The effects of VEGFR2 downstream signaling were examined to understand the mechanism underlying DKK1- induced angiogenesis in HUVECs. We found that DKK1 increased the expression of phosphorylated VEGFR2 (pVEGFR2) in a concentration-dependent manner. In addition, DKK1 significantly enhanced the expression of p-p70S6K in HUVECs whereas there was no increase in the protein level of mTOR in comparison to the control (Figure 2D). These data demonstrate that DKK1 might enhance the angiogenic potential of HUVECs through VEGFR2-mediated mTOR/p70S6K signaling *in vitro*.

Co-culture with Hep3B stable cells and stromal cells

To investigate whether DKK1 induces angiogenesis in HCC spheroids, we generated an MCTS. We confirmed a profound enhancement of spheroid compactness in MCTS generated using Hep3B wild-type cells, compared to the control (Figure 3A). IF staining of MCTS showed that DKK1 expression levels in MCTS generated using Hep3B wild-type cells were significantly higher than in those generated using Hep3B CRISPR#73 cells (Figure 3B). Expression of the endothelial cell marker, CD31, was enhanced in MCTS generated using Hep3B wild-type, compared to the control. In addition, expression levels of the mesenchymal ell markers, vimentin and Slug, were increased (all $P<0.01$), whereas expression of the epithelial cell marker, E-cadherin, was attenuated ($P<0.001$) in MCTS generated using Hep3B wild-type cells, compared to MCTS generated using Hep3B CRISPR#73 cells (Figure 3C). Akt activation, detected using phosphorylated-Akt [at Ser473] antibody, was increased to a greater extent in MCTS generated using Hep3B-wild type cells compared to MCTS generated using Hep3B CRISPR#73 cells (Figure 3D).

DKK1 promotes tumorigenesis in the xenograft mouse model

The xenograft mouse model was produced using Hep3B wild-type and CRISPR#73 cells to investigate whether DKK1 promotes tumorigenesis. Serum DKK1 levels were significantly higher in the model generated Hep3B wild-type cells than that generated using Hep3B CRISPR#73 cells (Supplement 3). Xenograft tumors generated using Hep3B CRISPR#73 cells (n=10) exhibited slower growth and smaller tumor volume/weight, than the controls (n=10) (Figures 4A-C).

Immunohistochemistry (IHC) staining showed that Ki-67 expression levels in xenograft tumors generated using Hep3B wild-type cells were slightly higher than those in xenograft tumors generated using Hep3B

CRISPR#73 cells (Figure 4D). These results indicate that DKK1 promotes HCC tumorigenesis by affecting tumor cell proliferation.

DKK1 promotes angiogenesis through epithelial-mesenchymal transition

To investigate the mechanism of HCC tumorigenesis by DKK1, we observed the angiogenesis and EMT of xenograft mouse models using IF study. IF staining of serial sections of xenograft tumors showed that DKK1 expression levels in xenograft tumors generated using Hep3B wild-type cells were significantly higher than in those generated using Hep3B CRISPR#73 (P<0.05). In addition, the expression of angiogenesis markers, VEGFR2 and CD31, in xenograft tumors generated using Hep3B wild-type cells were significantly higher than in those generated using Hep3B CRISPR#73 cells (all P<0.05) (Figures 5A-B). The expression levels of mesenchymal markers of vimentin (P<0.05) and fibronectin (P<0.01) were significantly attenuated in xenograft tumors generated using Hep3B CRISPR#73 cells, compared to the controls, whereas the expression of the epithelial marker, E-cadherin, was significantly enhanced (P<0.05) in xenograft tumors generated using Hep3B CRISPR#73 cells, compared to the controls (Figures 5C and 5D). These results suggest that DKK1 promotes angiogenesis through EMT in HCC.

DKK1 enhanced tumor growth and metastasis in the engineered mouse model.

Hydrodynamic injection was performed to investigate the tumorigenic potential of DKK1. We previously confirmed that HCC is induced by the co-expression of $HRAS^{G12V}$ with an shRNA downregulating p53 in the liver (30). To investigate the effects of DKK1 in the liver, we expressed DKK1 together with the aforementioned oncogenic combinations. The liver was harvested 5 weeks after hydrodynamic injection (Figure 6A). DKK1-2A-$HRAS^{G12V}$ + shp53 mice (HI_DKK1 mice) (n=5) had significantly more tumors with larger size than those of luciferase-2A-$HRAS^{G12V}$ + shp53 mice (HI_Luc2A mice) (n=5) (Figure 6B). IHC staining showed that HRAS expression levels were similar between the HI_DKK1 and HI_Luc2A groups and that Ki-67 staining of HI_DKK1 tumors was slightly higher than that of HI_Luc2A tumors (Figure 6C). The expression levels of DKK1 and the angiogenesis markers, VEGFR2 and CD31, were significantly higher in HI_DKK1 tumors than in HI_Luc2A tumors (all P<0.001) (Figures 6D-E). Expression levels of the epithelial marker, E-cadherin, was significantly attenuated and the mesenchymal markers of fibronectin were significantly enhanced in HI_DKK1 tumors, compared to the control (all P<0.001) (Figure 6F-G). These results indicate that DKK1 promotes angiogenesis through EMT in the mouse liver.

Discussion

We previously reported that DKK1 promotes angiogenesis via VEGFR2 regulation (27). However, the specific interaction between DKK1 and VEGFR2 in HCC remains to be ascertained. In this study, we first

confirmed that rDKK1 increases the invasion of HUVECs and then established stable cell lines with regulated DKK1 expression. Second, we found that the tube formation and migration abilities of HUVECs were significantly enhanced upon treatment with concentrated CM with high DKK1 concentration. Third, a signaling study showed that DKK1 was correlated with the VEGFR2-mediated mTOR/p70S6K signaling pathway. Fourth, we also found that DKK1 enhanced spheroid compactness and EMT in HCC-MCTS models. In addition, we reported that DKK1 promoted angiogenesis and tumorigenesis in xenograft tumor and mouse liver, which was supported by the increased expression of endothelial and EMT markers, such as CD31, vimentin, fibronectin and decreased expression of E-cadherin. Based on these results, we concluded that DKK1 promotes angiogenesis and tumorigenesis via upregulation of VEGFR2-mediated mTOR/p70S6K signaling and EMT.

Our study has several unique findings. First, our study provides additional support to the fact that DKK1 is significantly associated with angiogenesis of endothelial cells. To date, it has been reported that DKK1 promotes the angiogenic effects of endothelial cells and fibroblasts (31, 32). Smadja *et al.* (31) showed that DKK1 enhanced the proangiogenic potential of human endothelial colony-forming cells and these angiogenic effects have been attributed to enhancement of VEGFR2. In addition, Jiang *et al*. (33) showed that DKK1 is correlated with angiogenesis in fibroblasts through increased expression of VEGF and also found that HIF-1α may be associated with DKK1-induced HUVECs migration. Our data similarly found that DKK1 raised the angiogenic potential of endothelial cells, which was supported by the increased effects of HUVEC invasion, tube formation and migration. Our results showed that the angiogenic effects of HUVECs were increased by DKK1 in HCC cells.

Second, because we noticed a close association between DKK1 and angiogenesis, we focused on the mechanism involved. We found that DKK1 promoted HUVECs invasion and migration by upregulating VEGFR2-mediated mTOR/p70S6K pathway. mTOR expression is frequently upregulated in cancer, including HCC and is associated with poor prognosis, poorly differentiated tumors and early recurrence (34). In addition, Trinh *et al.* (35) determined that VEGF-A signaling acts on tumor cells as a stimulator of the Akt/mTOR pathway. Our results showed that DKK1 increased p-VEGFR2 and p-p70S6K protein levels in HUVECs. p70S6K, which is activated in signaling pathways that include mTOR, is significantly associated with HCC (36, 37). Li *et al*. (36) suggested that the expression level of p-p70S6K was increased in HCC compared to that in cirrhotic nodules and normal liver tissue using immunostaining. In addition, Kristine *et al*. (38) showed that patients with breast tumors having increased expression of p-p70S6K showed increased metastasis and worse disease-free survival. Based on these results, our data suggest that the DKK1-induced VEGFR2 downstream pathway is involved in the angiogenesis of endothelial cells. Considering that DKK1 is a major player in VEGFR2-mediated mTOR/p70S6K, DKK1 may be an attractive target for preventing the incidence of angiogenesis.

Third, we showed the influence of DKK1 on spheroid formation using Hep3B, HUVEC, LX2 and WI-38 cells. Our results reveal a striking correlation between the compactness ability of DKK1 and MCTS. In ovarian cancer cells, Katharine *et al.* (39) first indicated that a cell line possessing myofibroblast-like properties could form compact spheroids and subsequently, Katharine suggested that compact spheroid formation

may facilitate ovarian cancer cell invasion. In addition, Cho *et al.* (40) found that YAP/TAZ levels were significantly different for each type of HCC-MCTS model, while Hep3B MCTS had the highest level of YAP/TAZ expression. YAP and TAZ are known to contribute to cell cycle (41) and Jorgenson *et al.* (42) reported that TAZ activation is associated with fibroblast spheroid growth. In summary, although Kelm *et al.* (43) reported an inverse association between tumor cell spheroid cohesiveness and invasive potential, a positive correlation between tumorigenicity and spheroid formation of cancer cells has been suggested (44). Taken together, our MCTS results show that a DKK1-mediated increase in compactness, in addition to a rise in the expression levels of vimentin and Slug in MCTS, may promote cancer cell invasion. In addition, the relationship between YAP/TAZ and the ability of DKK1 including spheroid compactness should be further studied.

Fourth, we found that there was an increase in the expression of angiogenesis and EMT markers in the mouse model, indicating the enhancement of angiogenesis and EMT upon DKK1 stimulation. Similar to the findings of the present study, Yao *et al*. (45) showed that in vasculogenic mimicry, DKK1 increases the expression level of EMT-related protein in non-small cell lung cancer. In addition, Maha *et al*. (46) found that since DKK1 facilitates tumor invasion and migration through transforming growth factor beta 1, it may induce EMT in HCC cell lines. Indeed, increasing evidence indicates a central role of EMT, which might occur at the leading edge of tumor cells, under particular factors derived from the tumor microenvironment in HCC (47). In addition to EMT, DKK1 is significantly associated with endothelial-to-mesenchymal transition (EndMT) (27, 48). Previously, Choi *et al*. (27) found that DKK1 increases the expression of EndMT-related proteins (N-cadherin, Twist and vimentin) in endothelial cells and Cheng *et al.* (48) demonstrated that DKK1 enhances EndMT in aortic endothelial cells by augmenting ALK/Smad signaling to modulate the endothelial cell phenotype. In contrast, some studies have shown that EMT is negatively regulated by DKK1 (49–51). In spite of this controversy regarding the interaction between DKK1 and EMT/EndMT (52, 53), based on the findings of our current study, we postulate that DKK1 may help to develop effective therapies against HCC.

There are several limitations to this study. First, our data show that DKK1 activates VEGFR2 downstream signaling, but only at the endothelial cell level. The mechanism of DKK1 should be further investigated in the HCC cell line or HCC mouse model. Second, our data confirmed that DKK1 activates downstream molecules of VEGFR2 signaling, but further studies are required to determine the underlying mechanism. In addition, since DKK1 is known to be a Wnt signaling antagonist, it needs to be a studied whether the activation of VEGFR2 signaling by DKK1 is dependent or independent of Wnt signaling.

Conclusion

Our findings demonstrated that DKK1 facilitates endothelial cell angiogenesis through the upregulation of VEGFR2-mediated mTOR/p70S6K signaling and promotes HCC progression through the activation of EMT factors in diverse HCC models. Our results suggest that DKK1 is a potential therapeutic target for HCC.

Abbreviations

HCC: Hepatocellular carcinoma

VEGF: Vascular endothelial growth factor

FGF: Fibroblast growth factor

PDGF: Platelet-derived growth factor

VEGFRs: VEGF receptors

EMT: Epithelial-to-mesenchymal transition

DKK1: Dickkopf-1

MMP7: Metalloproteinase 7

mTOR: Mammalian target of rapamycin

p70S6K: p70 S6 kinase

HUVECs: Human umbilical vein endothelial cells

CRISPR-Cas9: Clustered regularly interspaced short palindromic repeats-associated nuclease 9

crRNA: CRISPR RNA

gRNA: Guide RNA

tracrRNA: Transactivating crRNA

ELISA: Enzyme-linked immunosorbent assay

H&E: Hematoxylin and eosin

CM: Conditioned medium

PI3K: Phosphoinositide 3-kinase

CD31: Cluster of differentiation 31

IHC: Immunohistochemistry

EnMT: Endothelial-to-mesenchymal transition

MCTSs: Multicellular tumor spheroids

Declarations

Ethics approval and consent to participate

Not applicable.

Consent for publication

Not applicable.

Availability of data and material

Data available upon request.

Competing interests

The authors declare that they have no competing interests.

Funding

This work was supported by the National Research Foundation of Korea (NRF) grant funded by the Korea government (MSIT) (no. 2019R1A2C4070136) and by a faculty research grant from Yonsei University College of Medicine (6-2018-0130).

Author contributions

Conception and design: SU; *Development of methodology*: SU, SH, HJ, HM, KJ ; *Experiment, analysis, and interpretation of data*: SH, HJ, HM, KJ, SU; *Writing, review, and/or revision of the manuscript*: SH, HJ, HM, KJ, HW, BK, JY, DY, SH, SU; *Administrative, technical, or material support*: SU ; *Study supervision*: SU. All authors read and approved the final manuscript.

Acknowledgements

The authors would like to express our gratitude to editage (https://app.editage.co.kr) for editing the English text of a draft of manuscript that greatly improved it.

References

1. Siegel R, Ward E, Brawley O, Jemal A. Cancer statistics, 2011: the impact of eliminating socioeconomic and racial disparities on premature cancer deaths. CA Cancer J Clin. 2011;61(4):212-36.
2. Liu K, Min XL, Peng J, Yang K, Yang L, Zhang XM. The Changes of HIF-1α and VEGF Expression After TACE in Patients With Hepatocellular Carcinoma. J Clin Med Res. 2016;8(4):297-302.
3. Hanahan D, Weinberg RA. Hallmarks of cancer: the next generation. Cell. 2011;144(5):646-74.
4. Semenza GL. Angiogenesis in ischemic and neoplastic disorders. Annu Rev Med. 2003;54:17-28.
5. Daher S, Massarwa M, Benson AA, Khoury T. Current and Future Treatment of Hepatocellular Carcinoma: An Updated Comprehensive Review. J Clin Transl Hepatol. 2018;6(1):69-78.
6. Kong L, Zhang X, Li C, Zhou L. Potential therapeutic targets and small molecular drugs for pediatric B-precursor acute lymphoblastic leukemia treatment based on microarray data. Oncol Lett. 2017;14(2):1543-9.
7. Arciero CA, Sigurdson ER. Liver-directed therapies for hepatocellular carcinoma. J Natl Compr Canc Netw. 2006;4(8):768-74.
8. Amini A, Masoumi Moghaddam S, Morris DL, Pourgholami MH. The critical role of vascular endothelial growth factor in tumor angiogenesis. Curr Cancer Drug Targets. 2012;12(1):23-43.
9. Yi ZY, Feng LJ, Xiang Z, Yao H. Vascular endothelial growth factor receptor-1 activation mediates epithelial to mesenchymal transition in hepatocellular carcinoma cells. J Invest Surg. 2011;24(2):67-76.
10. Glinka A, Wu W, Delius H, Monaghan AP, Blumenstock C, Niehrs C. Dickkopf-1 is a member of a new family of secreted proteins and functions in head induction. Nature. 1998;391(6665):357-62.
11. Fedi P, Bafico A, Nieto Soria A, Burgess WH, Miki T, Bottaro DP, et al. Isolation and biochemical characterization of the human Dkk-1 homologue, a novel inhibitor of mammalian Wnt signaling. J Biol Chem. 1999;274(27):19465-72.
12. Mao B, Wu W, Davidson G, Marhold J, Li M, Mechler BM, et al. Kremen proteins are Dickkopf receptors that regulate Wnt/beta-catenin signalling. Nature. 2002;417(6889):664-7.
13. Mao B, Wu W, Li Y, Hoppe D, Stannek P, Glinka A, et al. LDL-receptor-related protein 6 is a receptor for Dickkopf proteins. Nature. 2001;411(6835):321-5.
14. Mukhopadhyay M, Shtrom S, Rodriguez-Esteban C, Chen L, Tsukui T, Gomer L, et al. Dickkopf1 is required for embryonic head induction and limb morphogenesis in the mouse. Dev Cell. 2001;1(3):423-34.
15. Zorn AM. Wnt signalling: antagonistic Dickkopfs. Curr Biol. 2001;11(15):R592-5.
16. Thompson MD, Monga SP. WNT/beta-catenin signaling in liver health and disease. Hepatology. 2007;45(5):1298-305.
17. Hu M, Kurobe M, Jeong YJ, Fuerer C, Ghole S, Nusse R, et al. Wnt/beta-catenin signaling in murine hepatic transit amplifying progenitor cells. Gastroenterology. 2007;133(5):1579-91.

18. Choi HJ, Park H, Lee HW, Kwon YG. The Wnt pathway and the roles for its antagonists, DKKS, in angiogenesis. IUBMB Life. 2012;64(9):724-31.
19. Zhang B, Ma JX. Wnt pathway antagonists and angiogenesis. Protein Cell. 2010;1(10):898-906.
20. Tung EK, Mak CK, Fatima S, Lo RC, Zhao H, Zhang C, et al. Clinicopathological and prognostic significance of serum and tissue Dickkopf-1 levels in human hepatocellular carcinoma. Liver Int. 2011;31(10):1494-504.
21. Kwack MH, Hwang SY, Jang IS, Im SU, Kim JO, Kim MK, et al. Analysis of cellular changes resulting from forced expression of Dickkopf-1 in hepatocellular carcinoma cells. Cancer Res Treat. 2007;39(1):30-6.
22. Kim SU, Park JH, Kim HS, Lee JM, Lee HG, Kim H, et al. Serum Dickkopf-1 as a Biomarker for the Diagnosis of Hepatocellular Carcinoma. Yonsei Med J. 2015;56(5):1296-306.
23. Shen Q, Fan J, Yang XR, Tan Y, Zhao W, Xu Y, et al. Serum DKK1 as a protein biomarker for the diagnosis of hepatocellular carcinoma: a large-scale, multicentre study. Lancet Oncol. 2012;13(8):817-26.
24. Patil MA, Chua MS, Pan KH, Lin R, Lih CJ, Cheung ST, et al. An integrated data analysis approach to characterize genes highly expressed in hepatocellular carcinoma. Oncogene. 2005;24(23):3737-47.
25. Chen L, Li M, Li Q, Wang CJ, Xie SQ. DKK1 promotes hepatocellular carcinoma cell migration and invasion through β-catenin/MMP7 signaling pathway. Mol Cancer. 2013;12:157.
26. Tao YM, Liu Z, Liu HL. Dickkopf-1 (DKK1) promotes invasion and metastasis of hepatocellular carcinoma. Dig Liver Dis. 2013;45(3):251-7.
27. Choi SH, Kim H, Lee HG, Kim BK, Park JY, Kim DY, et al. Dickkopf-1 induces angiogenesis via VEGF receptor 2 regulation independent of the Wnt signaling pathway. Oncotarget. 2017;8(35):58974-84.
28. Song Y, Kim SH, Kim KM, Choi EK, Kim J, Seo HR. Activated hepatic stellate cells play pivotal roles in hepatocellular carcinoma cell chemoresistance and migration in multicellular tumor spheroids. Sci Rep. 2016;6:36750.
29. Tahergorabi Z, Khazaei M. A review on angiogenesis and its assays. Iran J Basic Med Sci. 2012;15(6):1110-26.
30. Ju HL, Ahn SH, Kim DY, Baek S, Chung SI, Seong J, et al. Investigation of oncogenic cooperation in simple liver-specific transgenic mouse models using noninvasive in vivo imaging. PLoS One. 2013;8(3):e59869.
31. Smadja DM, d'Audigier C, Weiswald LB, Badoual C, Dangles-Marie V, Mauge L, et al. The Wnt antagonist Dickkopf-1 increases endothelial progenitor cell angiogenic potential. Arterioscler Thromb Vasc Biol. 2010;30(12):2544-52.
32. Weng LH, Ko JY, Wang CJ, Sun YC, Wang FS. Dkk-1 promotes angiogenic responses and cartilage matrix proteinase secretion in synovial fibroblasts from osteoarthritic joints. Arthritis Rheum. 2012;64(10):3267-77.

33. Jiang SJ, Li W, Li YJ, Fang W, Long X. Dickkopf-related protein 1 induces angiogenesis by upregulating vascular endothelial growth factor in the synovial fibroblasts of patients with temporomandibular joint disorders. Mol Med Rep. 2015;12(4):4959-66.
34. Matter MS, Decaens T, Andersen JB, Thorgeirsson SS. Targeting the mTOR pathway in hepatocellular carcinoma: current state and future trends. J Hepatol. 2014;60(4):855-65.
35. Trinh XB, Tjalma WA, Vermeulen PB, Van den Eynden G, Van der Auwera I, Van Laere SJ, et al. The VEGF pathway and the AKT/mTOR/p70S6K1 signalling pathway in human epithelial ovarian cancer. Br J Cancer. 2009;100(6):971-8.
36. Li W, Tan D, Zhang Z, Liang JJ, Brown RE. Activation of Akt-mTOR-p70S6K pathway in angiogenesis in hepatocellular carcinoma. Oncol Rep. 2008;20(4):713-9.
37. Wang C, Cigliano A, Jiang L, Li X, Fan B, Pilo MG, et al. 4EBP1/eIF4E and p70S6K/RPS6 axes play critical and distinct roles in hepatocarcinogenesis driven by AKT and N-Ras proto-oncogenes in mice. Hepatology. 2015;61(1):200-13.
38. Klos KS, Wyszomierski SL, Sun M, Tan M, Zhou X, Li P, et al. ErbB2 increases vascular endothelial growth factor protein synthesis via activation of mammalian target of rapamycin/p70S6K leading to increased angiogenesis and spontaneous metastasis of human breast cancer cells. Cancer Res. 2006;66(4):2028-37.
39. Sodek KL, Ringuette MJ, Brown TJ. Compact spheroid formation by ovarian cancer cells is associated with contractile behavior and an invasive phenotype. Int J Cancer. 2009;124(9):2060-70.
40. PE-162 : Establishment of 3D Multicellular Tumor Spheroids (MCTS) using Hepatocellular Carcinoma and Stromal cells for Screening Anti-cancer Therapeutic Agents. □·□□ □□□□ (KASL). 2018;2018(1):208-9.
41. Piccolo S, Dupont S, Cordenonsi M. The biology of YAP/TAZ: hippo signaling and beyond. Physiol Rev. 2014;94(4):1287-312.
42. Jorgenson AJ, Choi KM, Sicard D, Smith KM, Hiemer SE, Varelas X, et al. TAZ activation drives fibroblast spheroid growth, expression of profibrotic paracrine signals, and context-dependent ECM gene expression. Am J Physiol Cell Physiol. 2017;312(3):C277-c85.
43. Kelm JM, Timmins NE, Brown CJ, Fussenegger M, Nielsen LK. Method for generation of homogeneous multicellular tumor spheroids applicable to a wide variety of cell types. Biotechnol Bioeng. 2003;83(2):173-80.
44. Casey RC, Burleson KM, Skubitz KM, Pambuccian SE, Oegema TR, Jr., Ruff LE, et al. Beta 1-integrins regulate the formation and adhesion of ovarian carcinoma multicellular spheroids. Am J Pathol. 2001;159(6):2071-80.
45. Yao L, Zhang D, Zhao X, Sun B, Liu Y, Gu Q, et al. Dickkopf-1-promoted vasculogenic mimicry in non-small cell lung cancer is associated with EMT and development of a cancer stem-like cell phenotype. J Cell Mol Med. 2016;20(9):1673-85.
46. Fezza M, Moussa M, Aoun R, Haber R, Hilal G. DKK1 promotes hepatocellular carcinoma inflammation, migration and invasion: Implication of TGF-β1. PLoS One. 2019;14(9):e0223252.

47. Giannelli G, Koudelkova P, Dituri F, Mikulits W. Role of epithelial to mesenchymal transition in hepatocellular carcinoma. J Hepatol. 2016;65(4):798-808.
48. Cheng SL, Shao JS, Behrmann A, Krchma K, Towler DA. Dkk1 and MSX2-Wnt7b signaling reciprocally regulate the endothelial-mesenchymal transition in aortic endothelial cells. Arterioscler Thromb Vasc Biol. 2013;33(7):1679-89.
49. DiMeo TA, Anderson K, Phadke P, Fan C, Perou CM, Naber S, et al. A novel lung metastasis signature links Wnt signaling with cancer cell self-renewal and epithelial-mesenchymal transition in basal-like breast cancer. Cancer Res. 2009;69(13):5364-73.
50. Mitra A, Menezes ME, Shevde LA, Samant RS. DNAJB6 induces degradation of beta-catenin and causes partial reversal of mesenchymal phenotype. J Biol Chem. 2010;285(32):24686-94.
51. Menezes ME, Devine DJ, Shevde LA, Samant RS. Dickkopf1: a tumor suppressor or metastasis promoter? Int J Cancer. 2012;130(7):1477-83.
52. Potenta S, Zeisberg E, Kalluri R. The role of endothelial-to-mesenchymal transition in cancer progression. Br J Cancer. 2008;99(9):1375-9.
53. Thompson EW, Newgreen DF, Tarin D. Carcinoma invasion and metastasis: a role for epithelial-mesenchymal transition? Cancer Res. 2005;65(14):5991-5; discussion 5.

Figures

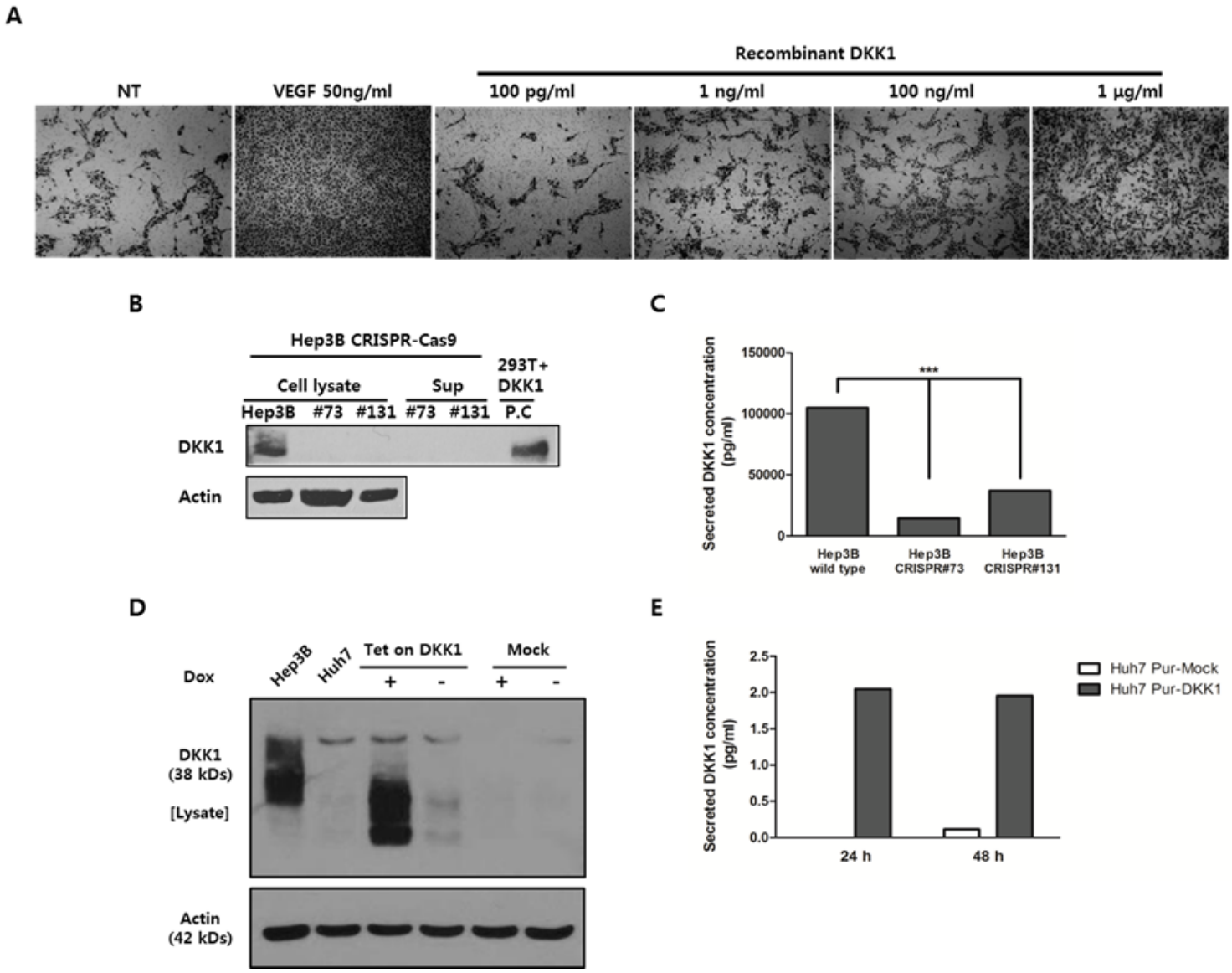

Figure 1

Regulation of DKK1 gene expression in Hep3B and Huh7 cells. (A) Effects of DKK1 on invasion assay in HUVECs. HUVECs were treated with the indicated concentration of rDKK1 and 50 ng/mL VEGF (as a positive control). (B) Western blot analysis of aggregated proteins, collected using centrifugation from Hep3B wild-type (Hep3B), Hep3B CRISPR#73 (#73) and Hep3B CRISPR#131 (#131) cells. DKK1-transfected HEK 293T cells were used as a positive control. Pellet: the aggregated fraction after centrifugation; sup: the supernatant (soluble fraction). (C) Protein levels of secreted DKK1 from Hep3B, #73 and #131 cells were measured using ELISA. (D) Western blot analysis of aggregated proteins from Huh7 Pur-DKK1, Huh7 Pur-Mock, Hep3B and Huh7 wild-type (Huh7) cells. Huh7 Pur-DKK1 and Huh7 Pur-Mock cells were cultured in the absence or presence of doxycycline (100 ng/mL) at 37°C for 48 h. Hep3B cells were used as a positive control for DKK1. (E) Secreted DKK1 protein levels of Huh7 Pur-DKK1 and HuH7 Pur-Mock cells were measured using ELISA after incubation with doxycycline (100 ng/mL) for 24 and 48 h.

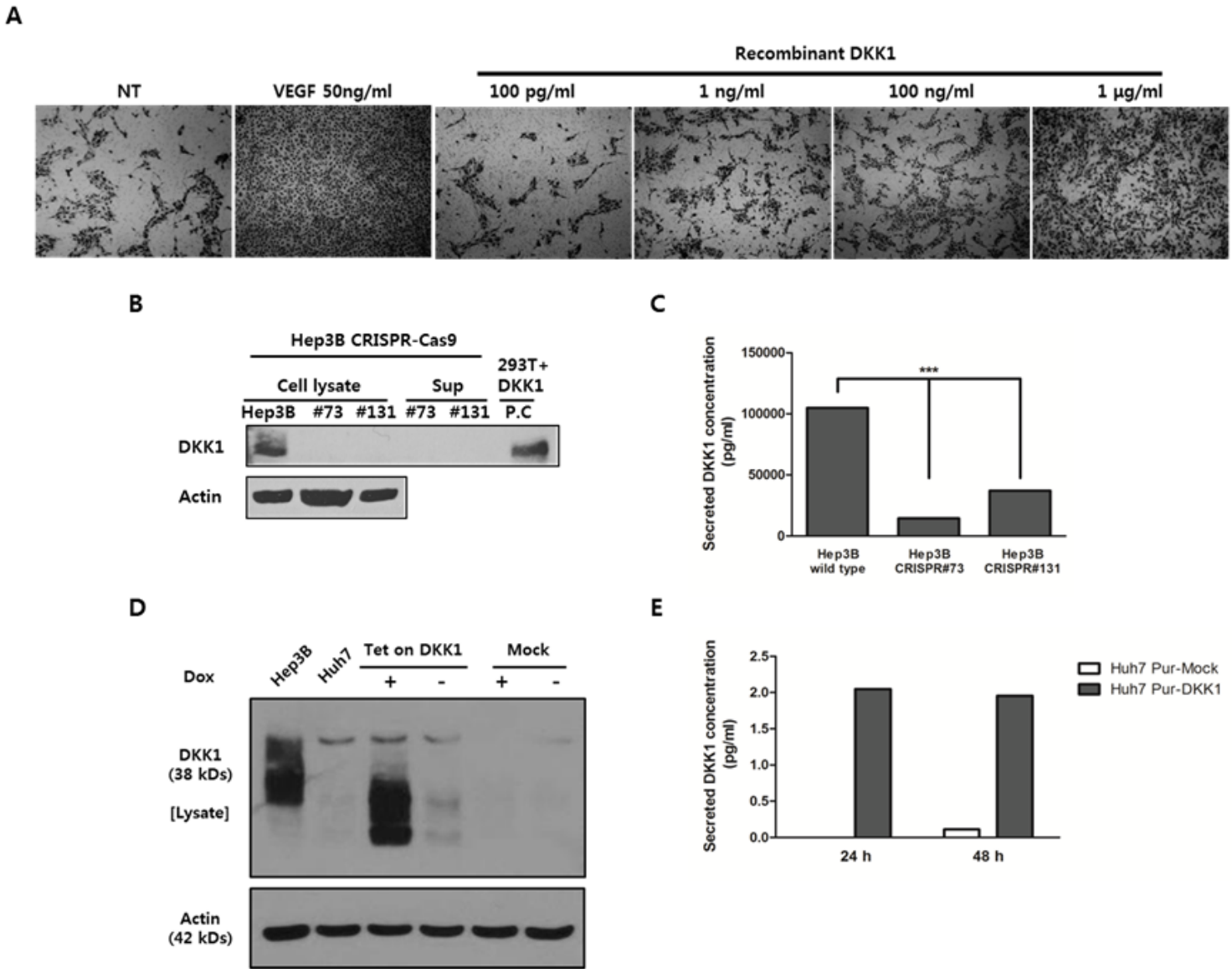

Figure 1

Regulation of DKK1 gene expression in Hep3B and Huh7 cells. (A) Effects of DKK1 on invasion assay in HUVECs. HUVECs were treated with the indicated concentration of rDKK1 and 50 ng/mL VEGF (as a positive control). (B) Western blot analysis of aggregated proteins, collected using centrifugation from Hep3B wild-type (Hep3B), Hep3B CRISPR#73 (#73) and Hep3B CRISPR#131 (#131) cells. DKK1-transfected HEK 293T cells were used as a positive control. Pellet: the aggregated fraction after centrifugation; sup: the supernatant (soluble fraction). (C) Protein levels of secreted DKK1 from Hep3B, #73 and #131 cells were measured using ELISA. (D) Western blot analysis of aggregated proteins from Huh7 Pur-DKK1, Huh7 Pur-Mock, Hep3B and Huh7 wild-type (Huh7) cells. Huh7 Pur-DKK1 and Huh7 Pur-Mock cells were cultured in the absence or presence of doxycycline (100 ng/mL) at 37°C for 48 h. Hep3B cells were used as a positive control for DKK1. (E) Secreted DKK1 protein levels of Huh7 Pur-DKK1 and HuH7 Pur-Mock cells were measured using ELISA after incubation with doxycycline (100 ng/mL) for 24 and 48 h.

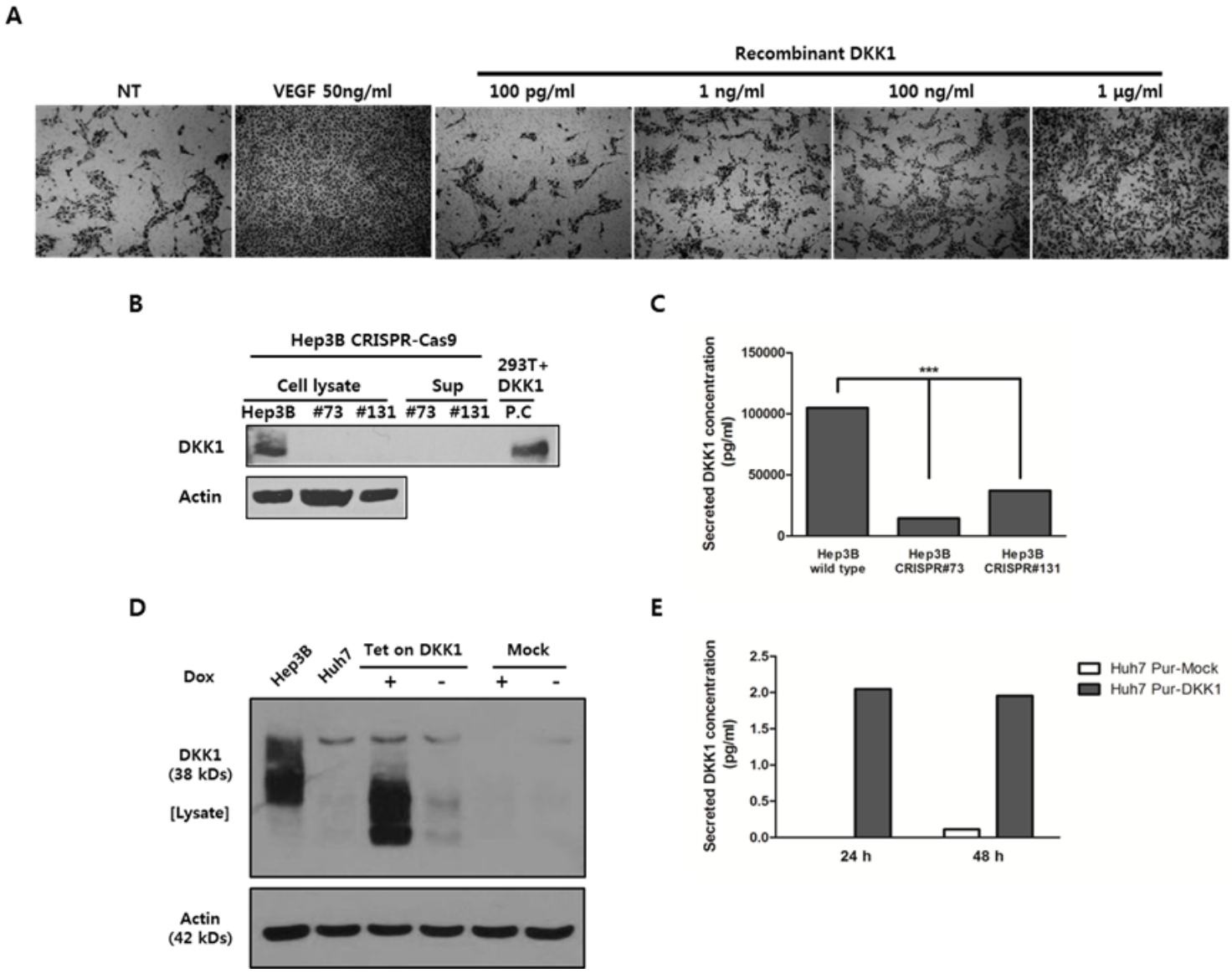

Figure 1

Regulation of DKK1 gene expression in Hep3B and Huh7 cells. (A) Effects of DKK1 on invasion assay in HUVECs. HUVECs were treated with the indicated concentration of rDKK1 and 50 ng/mL VEGF (as a positive control). (B) Western blot analysis of aggregated proteins, collected using centrifugation from Hep3B wild-type (Hep3B), Hep3B CRISPR#73 (#73) and Hep3B CRISPR#131 (#131) cells. DKK1-transfected HEK 293T cells were used as a positive control. Pellet: the aggregated fraction after centrifugation; sup: the supernatant (soluble fraction). (C) Protein levels of secreted DKK1 from Hep3B, #73 and #131 cells were measured using ELISA. (D) Western blot analysis of aggregated proteins from Huh7 Pur-DKK1, Huh7 Pur-Mock, Hep3B and Huh7 wild-type (Huh7) cells. Huh7 Pur-DKK1 and Huh7 Pur-Mock cells were cultured in the absence or presence of doxycycline (100 ng/mL) at 37°C for 48 h. Hep3B cells were used as a positive control for DKK1. (E) Secreted DKK1 protein levels of Huh7 Pur-DKK1 and HuH7 Pur-Mock cells were measured using ELISA after incubation with doxycycline (100 ng/mL) for 24 and 48 h.

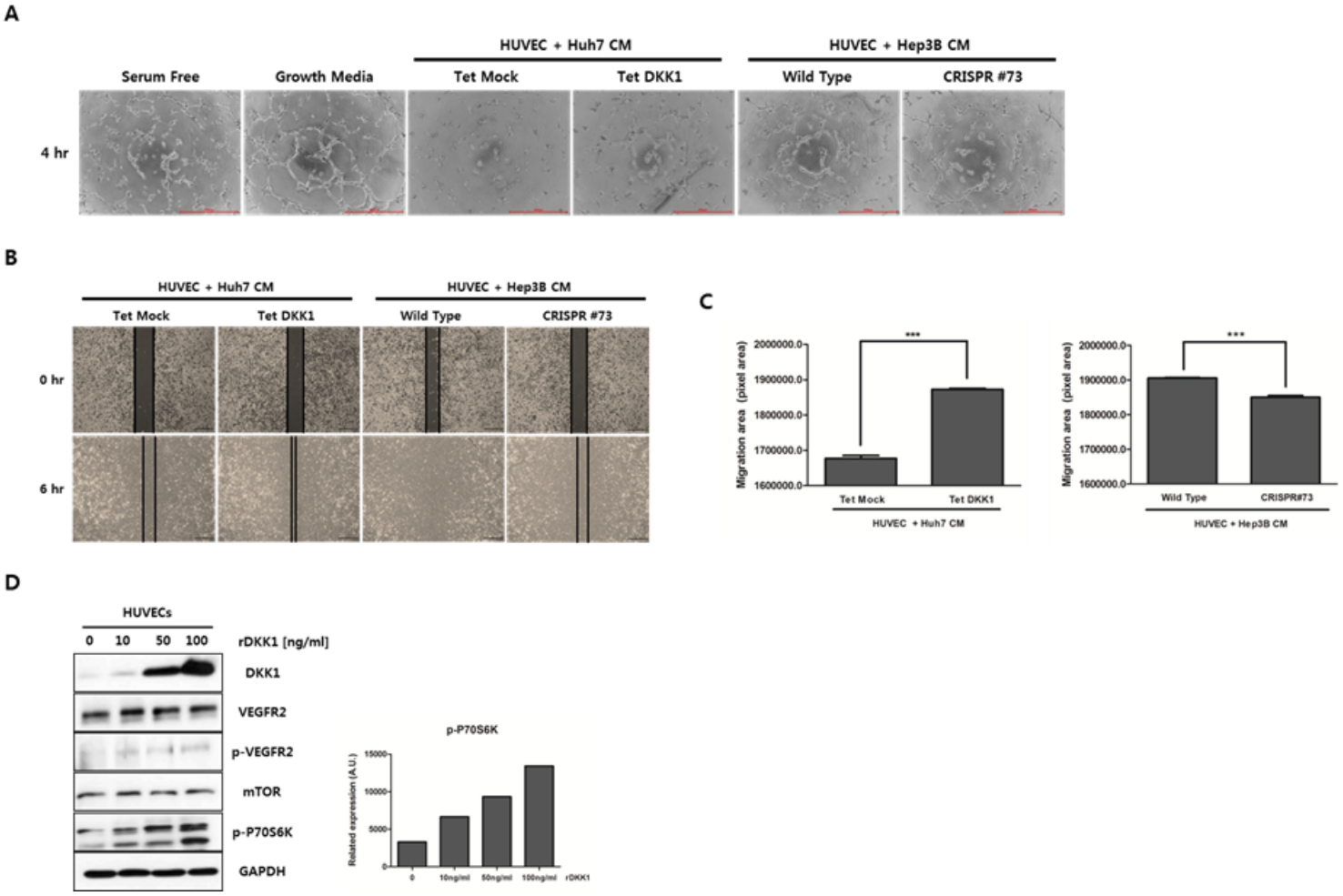

Figure 2

DKK1 increases the angiogenic effects of HUVECs. (A) Effects of DKK1 exposure on tube formation in HUVECs. HUVECs were cultured in serum free media (negative control), growth media (positive control) and concentrated CM of Huh7 Pur-Mock, Huh7 Pur-DKK1, Hep3B wild-type and Hep3B CRISPR#73 cells (scale bar: 500 μm). Concentrated CM was harvested from Huh7 Pur-DKK1 and Pur-Mock cells 24 h after doxycycline treatment (100 ng/mL). (B) Effects of DKK1 exposure on migration. HUVECs were cultured in concentrated CM from Huh7 Pur-Mock, Huh7 Pur-DKK1, Hep3B wild-type and Hep3B CRISPR#73 cells. Concentrated CM from Huh7 Pur-DKK1 and Huh7 Pur-Mock cells was harvested 24 h after doxycycline treatment (100 ng/mL). (C) Graphs show wound size (all $P<0.001$). (D) Lysates of control HUVECs, HUVECs + 10 ng/mL rDKK1, HUVECs + 50 ng/ml rDKK1 and HUVECs + 100 ng/ml rDKK1 cells were probed with the indicated antibodies. GAPDH was used as a loading control.

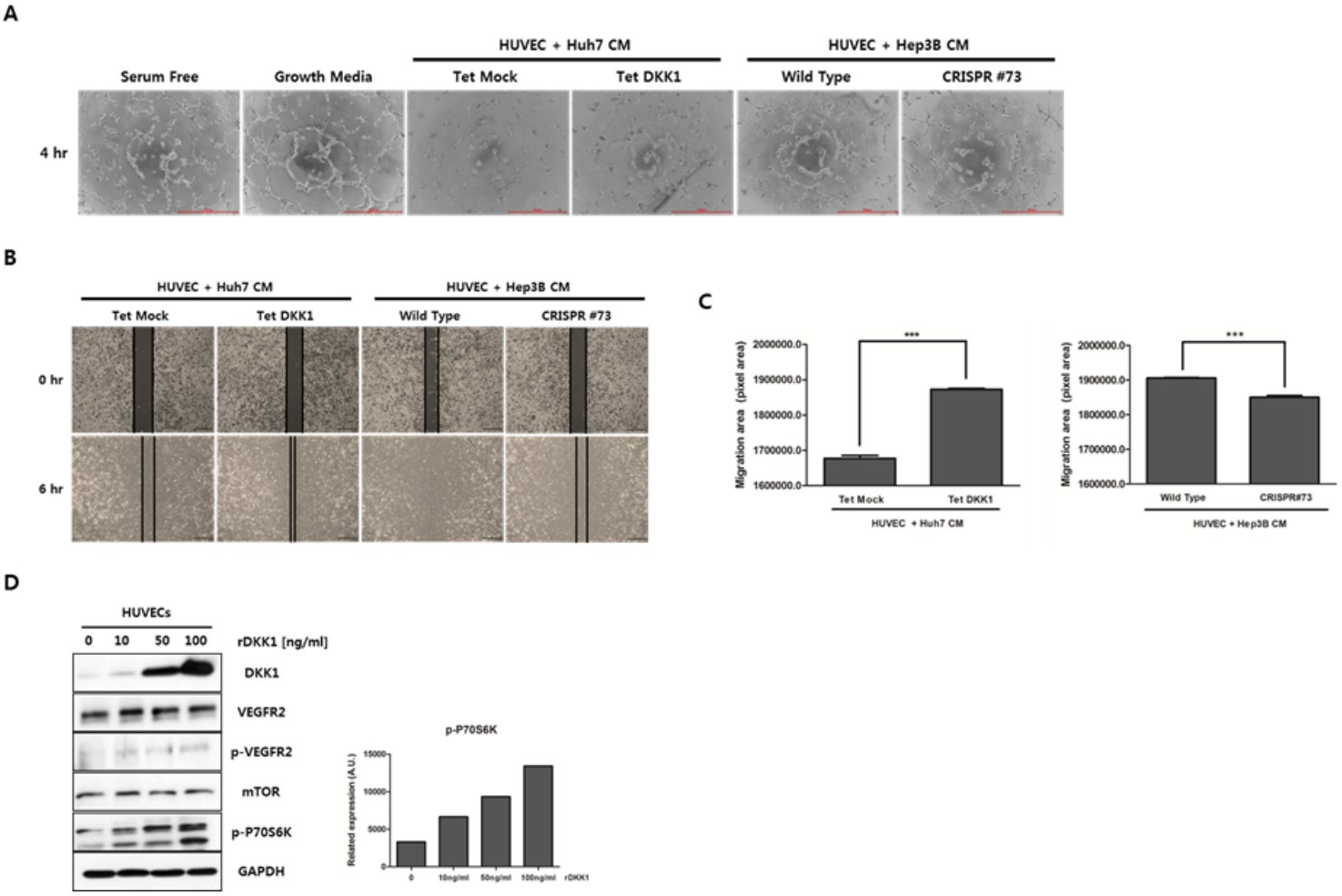

Figure 2

DKK1 increases the angiogenic effects of HUVECs. (A) Effects of DKK1 exposure on tube formation in HUVECs. HUVECs were cultured in serum free media (negative control), growth media (positive control) and concentrated CM of Huh7 Pur-Mock, Huh7 Pur-DKK1, Hep3B wild-type and Hep3B CRISPR#73 cells (scale bar: 500 μm). Concentrated CM was harvested from Huh7 Pur-DKK1 and Pur-Mock cells 24 h after doxycycline treatment (100 ng/mL). (B) Effects of DKK1 exposure on migration. HUVECs were cultured in concentrated CM from Huh7 Pur-Mock, Huh7 Pur-DKK1, Hep3B wild-type and Hep3B CRISPR#73 cells. Concentrated CM from Huh7 Pur-DKK1 and Huh7 Pur-Mock cells was harvested 24 h after doxycycline treatment (100 ng/mL). (C) Graphs show wound size (all $P<0.001$). (D) Lysates of control HUVECs, HUVECs + 10 ng/mL rDKK1, HUVECs + 50 ng/ml rDKK1 and HUVECs + 100 ng/ml rDKK1 cells were probed with the indicated antibodies. GAPDH was used as a loading control.

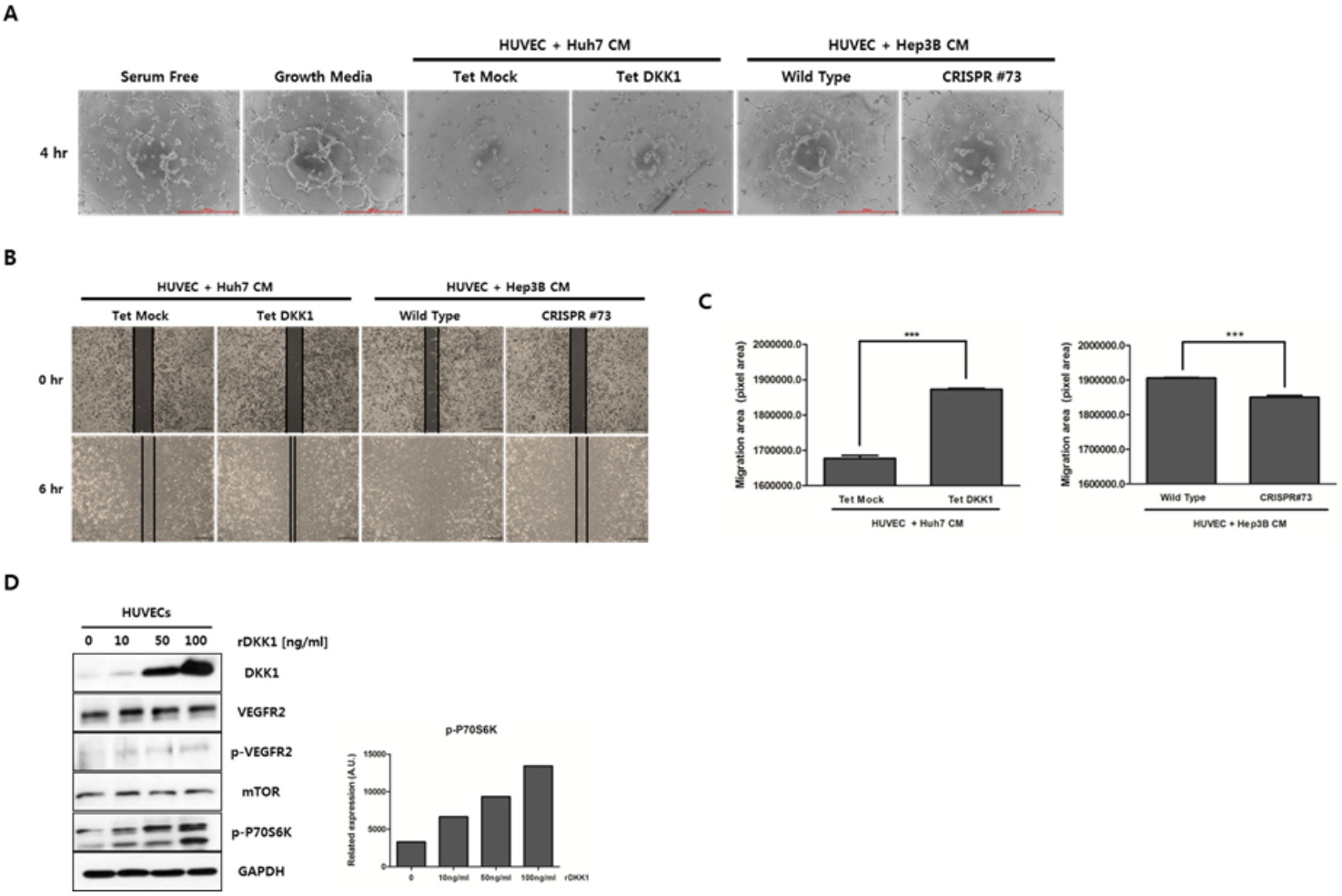

Figure 2

DKK1 increases the angiogenic effects of HUVECs. (A) Effects of DKK1 exposure on tube formation in HUVECs. HUVECs were cultured in serum free media (negative control), growth media (positive control) and concentrated CM of Huh7 Pur-Mock, Huh7 Pur-DKK1, Hep3B wild-type and Hep3B CRISPR#73 cells (scale bar: 500 μm). Concentrated CM was harvested from Huh7 Pur-DKK1 and Pur-Mock cells 24 h after doxycycline treatment (100 ng/mL). (B) Effects of DKK1 exposure on migration. HUVECs were cultured in concentrated CM from Huh7 Pur-Mock, Huh7 Pur-DKK1, Hep3B wild-type and Hep3B CRISPR#73 cells. Concentrated CM from Huh7 Pur-DKK1 and Huh7 Pur-Mock cells was harvested 24 h after doxycycline treatment (100 ng/mL). (C) Graphs show wound size (all $P<0.001$). (D) Lysates of control HUVECs, HUVECs + 10 ng/mL rDKK1, HUVECs + 50 ng/ml rDKK1 and HUVECs + 100 ng/ml rDKK1 cells were probed with the indicated antibodies. GAPDH was used as a loading control.

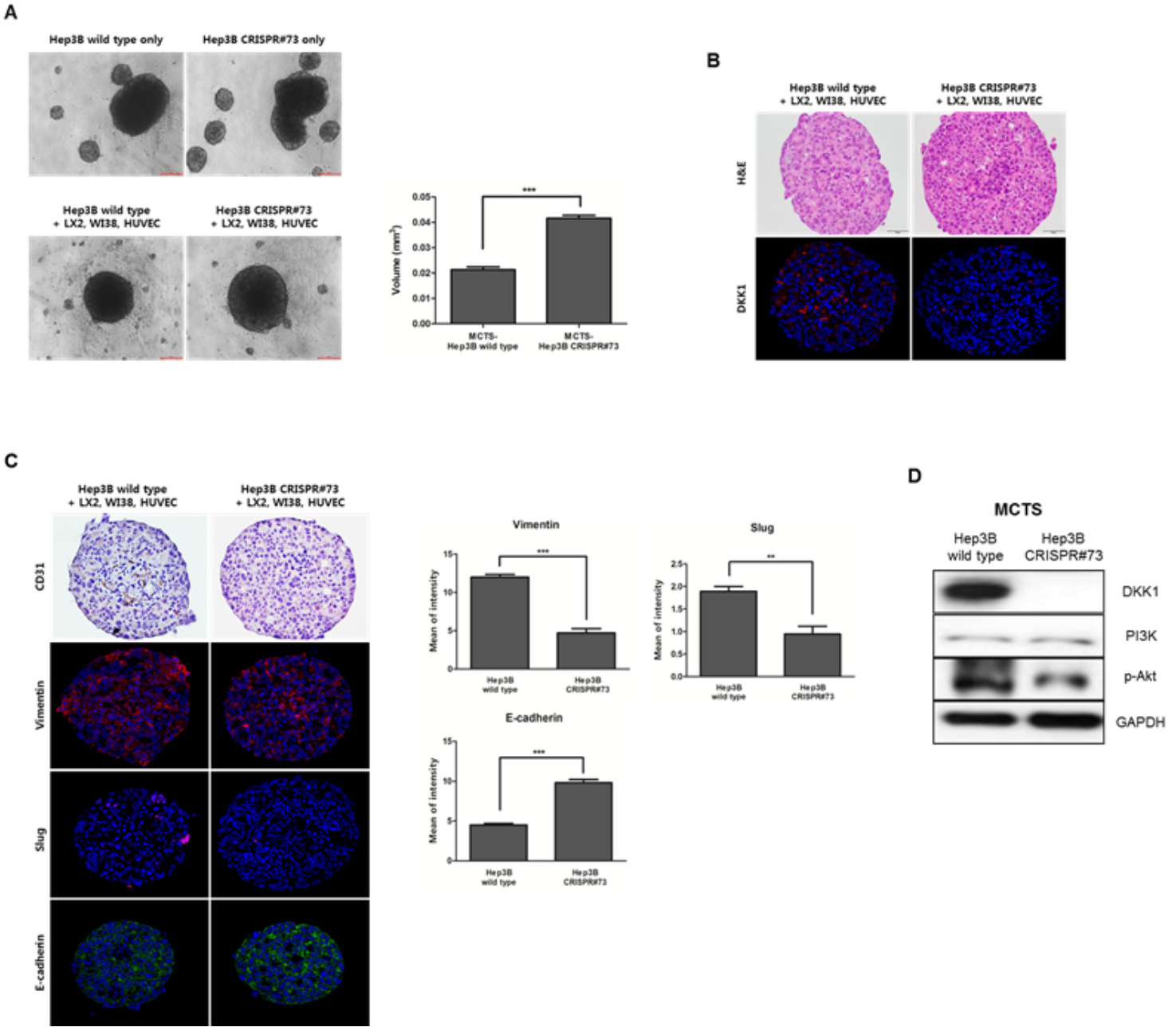

Figure 3

DKK1 enhanced the compactness and angiogenic effects of HCC-MCTS. (A) Hep3B wild-type and CRISPR#73 cells were co-cultured with or without stromal cells (HUVECs: LX2: WI38) for 3 days (scale bar: 200 μm). To calculate the volume of the spheroids, the radius of spheroids of the Hep3B wild-type and CRISPR#73 cells co-cultured with stromal cells were measured (P<0.001) (right panel). (B) H&E (scale bar: 50 μm) and IF staining (magnification, 200×) for DKK1 on the paraffin sections of HCC-MCTS. (C) IHC and IF staining for CD31, vimentin, Slug, and E-cadherin on serial paraffin sections of HCC-MCTS (magnification, 200×). (D) Lysates of MCTS generated using Hep3B wild-type and CRISPR#73 cells were probed with the indicated antibodies. GAPDH was used as a loading control.

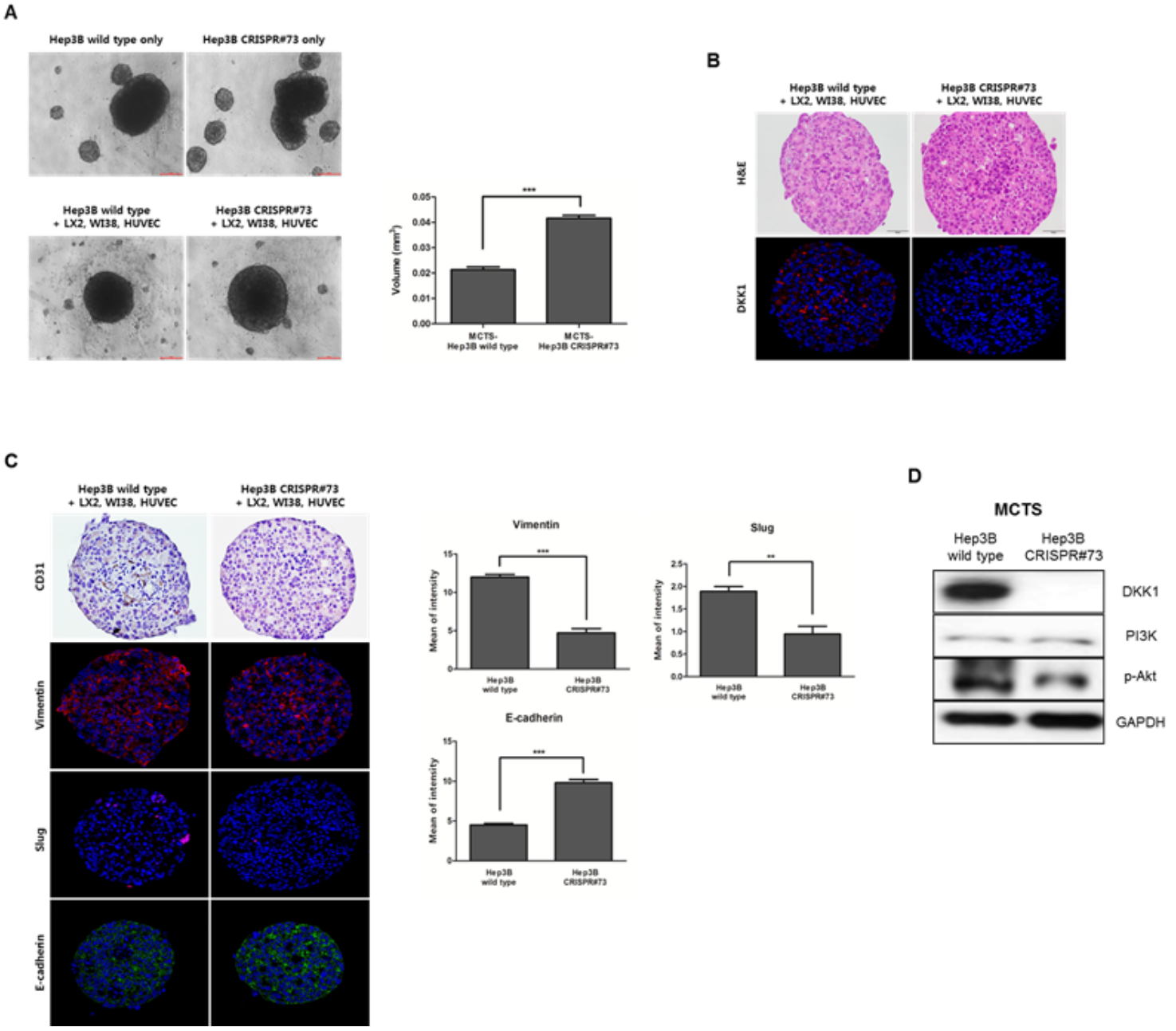

Figure 3

DKK1 enhanced the compactness and angiogenic effects of HCC-MCTS. (A) Hep3B wild-type and CRISPR#73 cells were co-cultured with or without stromal cells (HUVECs: LX2: WI38) for 3 days (scale bar: 200 μm). To calculate the volume of the spheroids, the radius of spheroids of the Hep3B wild-type and CRISPR#73 cells co-cultured with stromal cells were measured (P<0.001) (right panel). (B) H&E (scale bar: 50 μm) and IF staining (magnification, 200×) for DKK1 on the paraffin sections of HCC-MCTS. (C) IHC and IF staining for CD31, vimentin, Slug, and E-cadherin on serial paraffin sections of HCC-MCTS (magnification, 200×). (D) Lysates of MCTS generated using Hep3B wild-type and CRISPR#73 cells were probed with the indicated antibodies. GAPDH was used as a loading control.

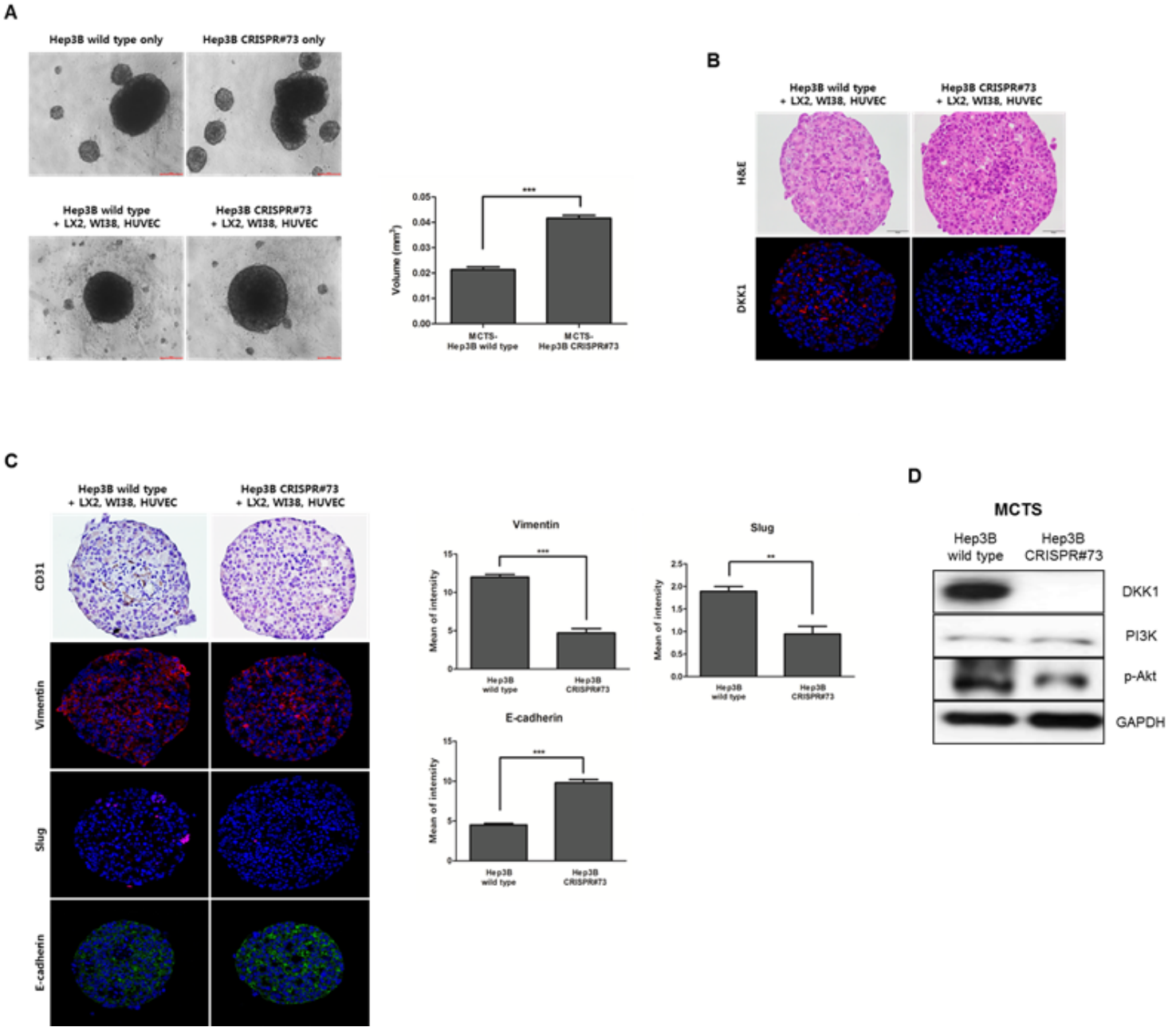

Figure 3

DKK1 enhanced the compactness and angiogenic effects of HCC-MCTS. (A) Hep3B wild-type and CRISPR#73 cells were co-cultured with or without stromal cells (HUVECs: LX2: WI38) for 3 days (scale bar: 200 μm). To calculate the volume of the spheroids, the radius of spheroids of the Hep3B wild-type and CRISPR#73 cells co-cultured with stromal cells were measured (P<0.001) (right panel). (B) H&E (scale bar: 50 μm) and IF staining (magnification, 200×) for DKK1 on the paraffin sections of HCC-MCTS. (C) IHC and IF staining for CD31, vimentin, Slug, and E-cadherin on serial paraffin sections of HCC-MCTS (magnification, 200×). (D) Lysates of MCTS generated using Hep3B wild-type and CRISPR#73 cells were probed with the indicated antibodies. GAPDH was used as a loading control.

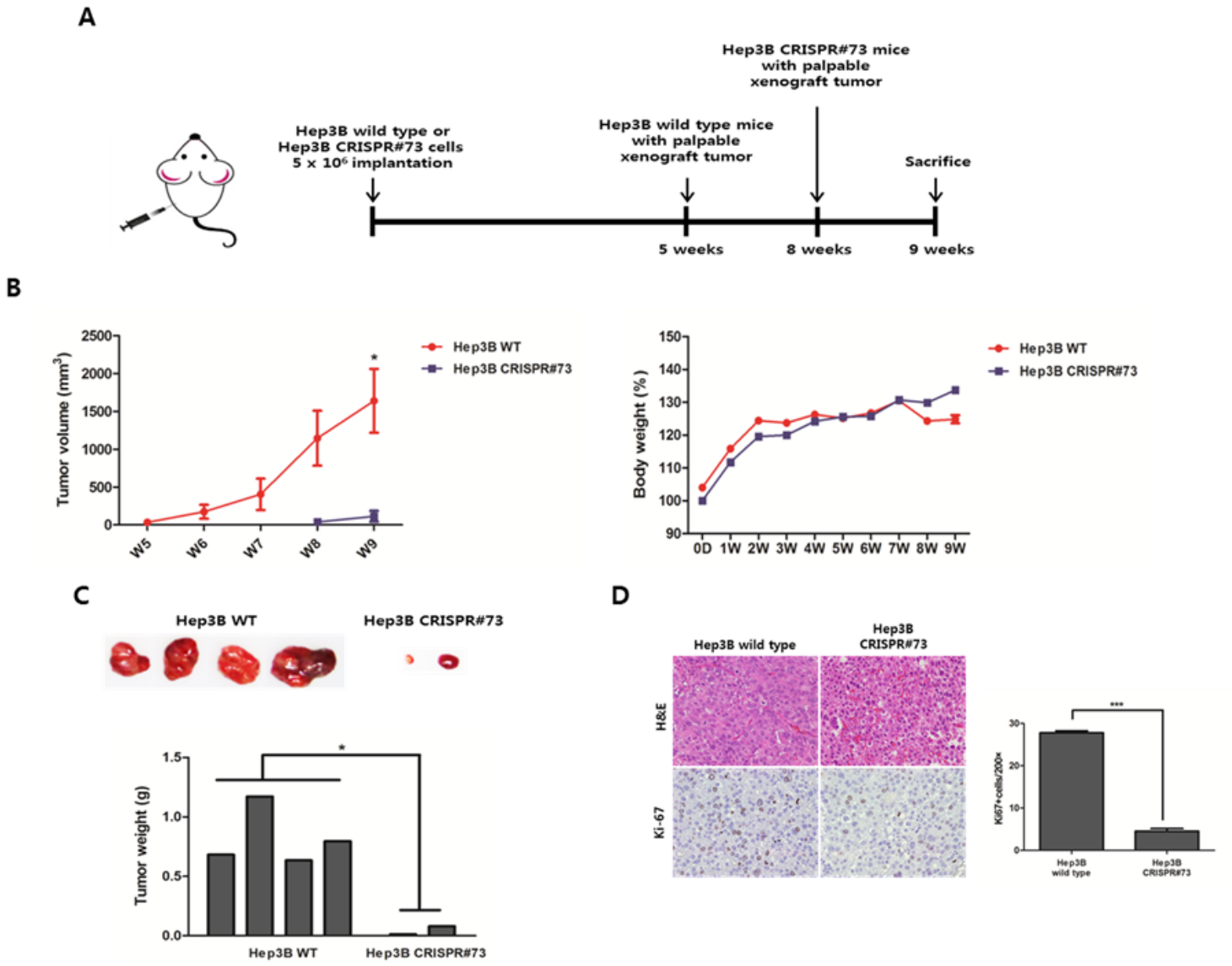

Figure 4

DKK1 increased tumorigenesis in the xenograft mouse model. (A) Xenograft tumors generated using Hep3B CRISPR#73 cells exhibited slower growth, (B) smaller tumor volume and (C) smaller tumor weight ($P<0.01$) ($n=10$) than, the controls. (D) H&E (magnification, 200x) and IHC staining (magnification, 400x) for Ki-67 on serial paraffin sections of Hep3B wild-type and CRISPR#73 tumors. Graph of Ki-67 positive Hep3B stable cells ($P<0.001$).

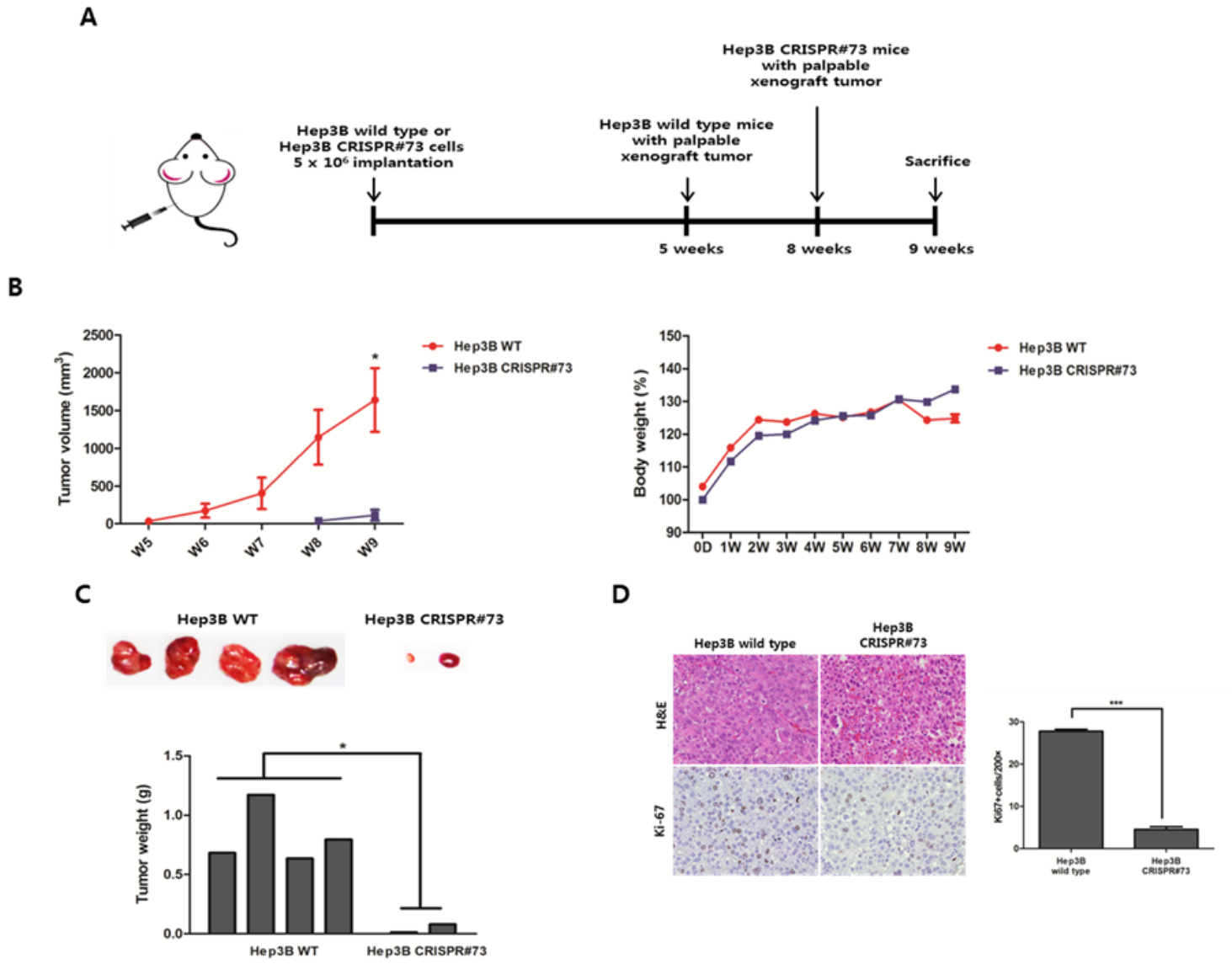

Figure 4

DKK1 increased tumorigenesis in the xenograft mouse model. (A) Xenograft tumors generated using Hep3B CRISPR#73 cells exhibited slower growth, (B) smaller tumor volume and (C) smaller tumor weight ($P<0.01$) ($n=10$) than, the controls. (D) H&E (magnification, 200x) and IHC staining (magnification, 400x) for Ki-67 on serial paraffin sections of Hep3B wild-type and CRISPR#73 tumors. Graph of Ki-67 positive Hep3B stable cells ($P<0.001$).

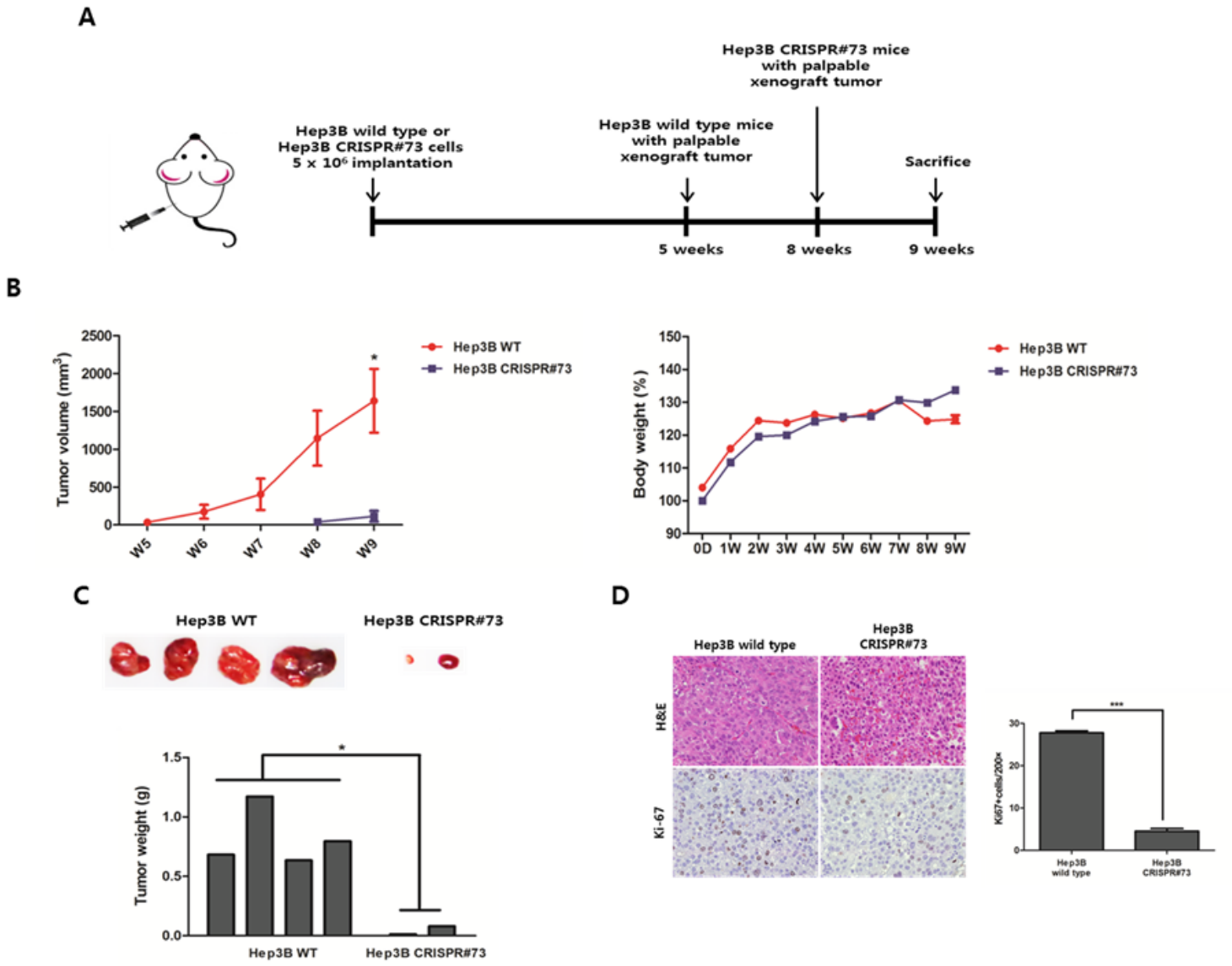

Figure 4

DKK1 increased tumorigenesis in the xenograft mouse model. (A) Xenograft tumors generated using Hep3B CRISPR#73 cells exhibited slower growth, (B) smaller tumor volume and (C) smaller tumor weight ($P<0.01$) ($n=10$) than, the controls. (D) H&E (magnification, 200x) and IHC staining (magnification, 400x) for Ki-67 on serial paraffin sections of Hep3B wild-type and CRISPR#73 tumors. Graph of Ki-67 positive Hep3B stable cells ($P<0.001$).

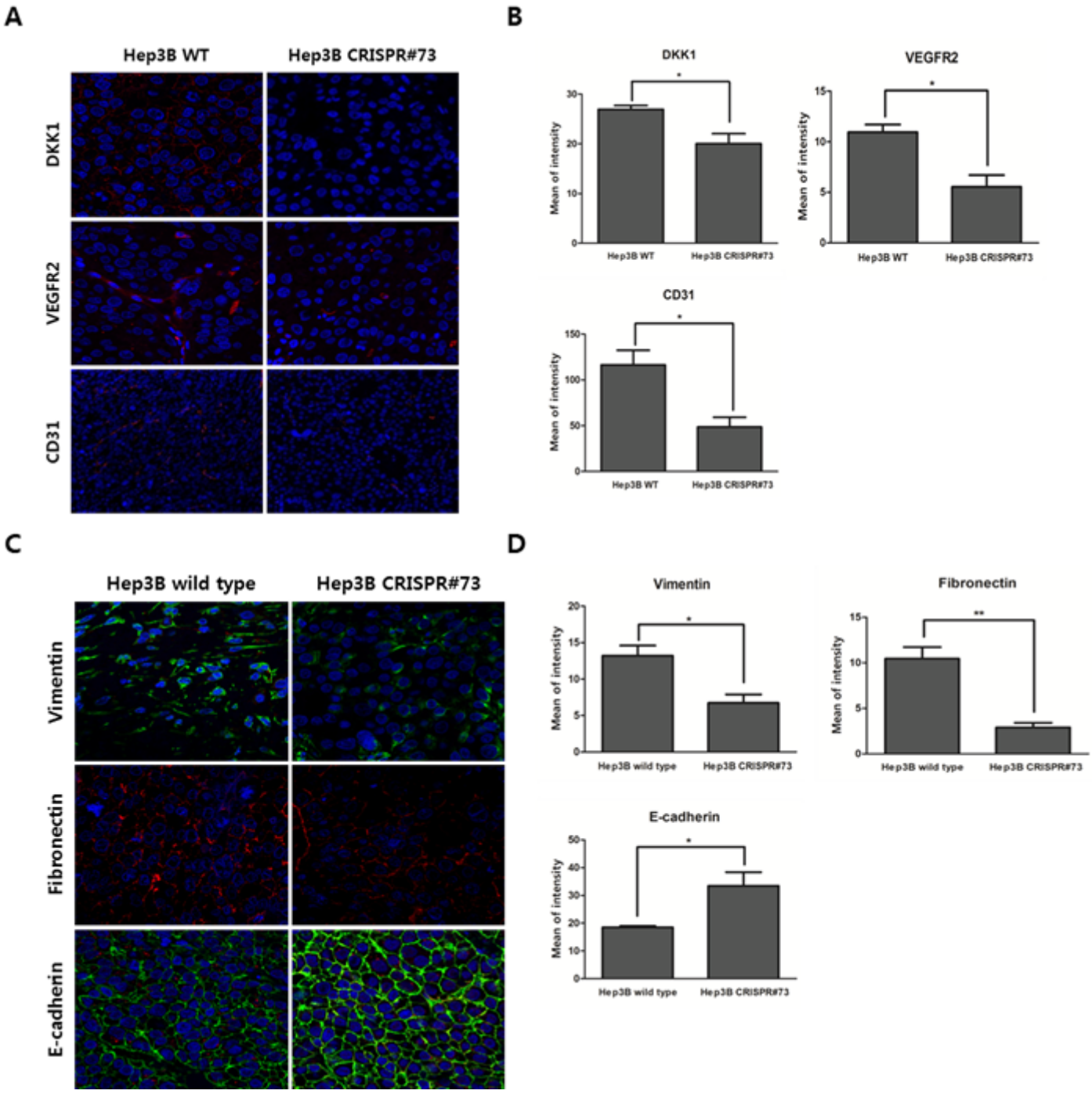

Figure 5

DKK1 increased angiogenesis and metastasis in the xenograft mouse model. (A) Observation of IF staining for DKK1, VEGFR2 and CD31 on serial paraffin sections of xenograft tumors generated using Hep3B wild-type and CRISPR#73 with confocal microscopy. (B) Quantification of DKK1 ($P<0.05$), VEGFR2 ($P<0.05$) and CD31 ($P<0.05$) IF, presented as the mean fluorescence intensity. (C) Observation of IF staining for vimentin, fibronectin and E-cadherin on serial paraffin sections of xenograft tumors generated using Hep3B wild-type and CRISPR#73 cells with confocal microscopy. (D) Quantification of vimentin ($P<0.05$), fibronectin ($P<0.01$) and E-cadherin ($P<0.05$) IF, presented as the mean fluorescence intensity.

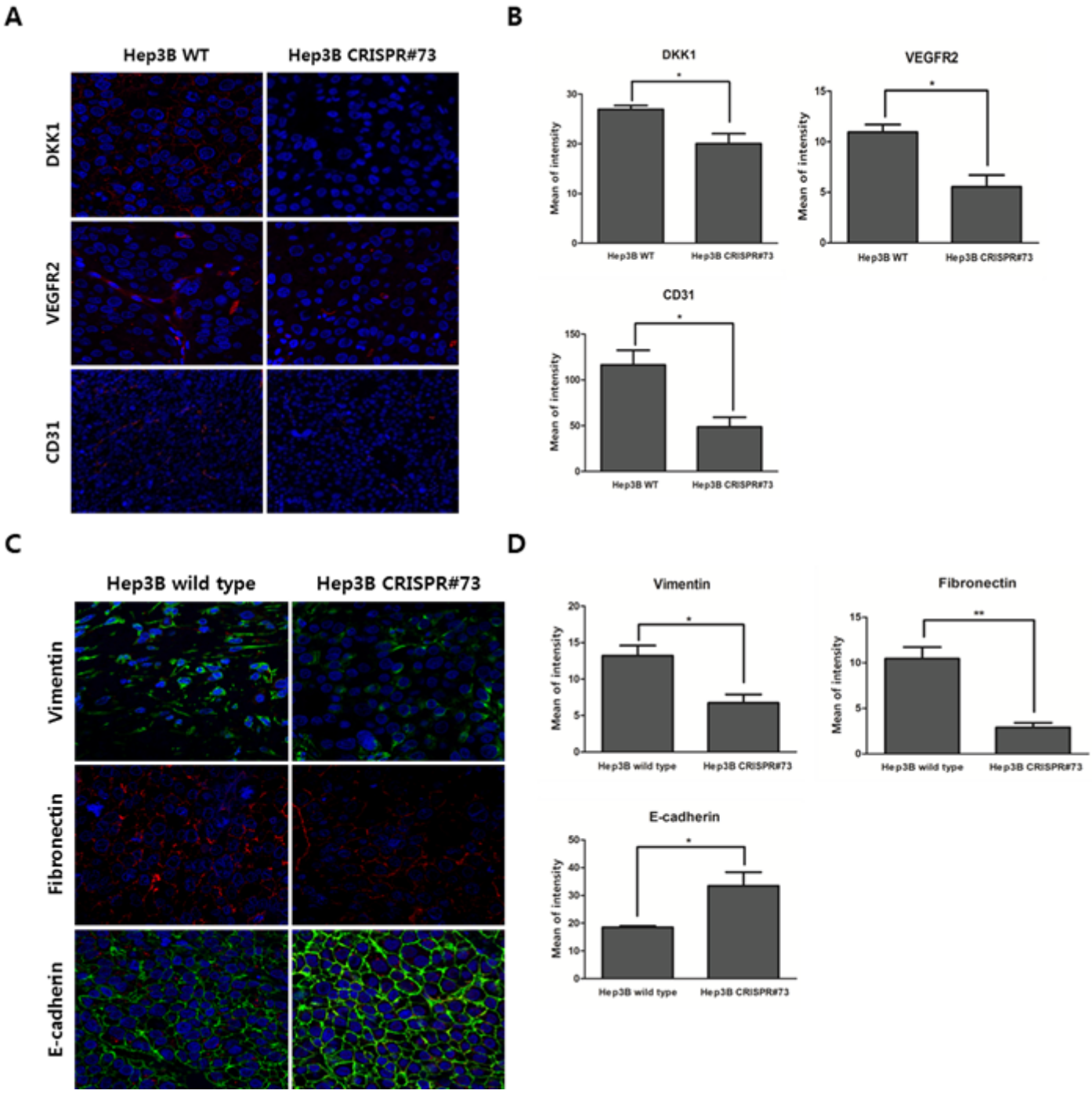

Figure 5

DKK1 increased angiogenesis and metastasis in the xenograft mouse model. (A) Observation of IF staining for DKK1, VEGFR2 and CD31 on serial paraffin sections of xenograft tumors generated using Hep3B wild-type and CRISPR#73 with confocal microscopy. (B) Quantification of DKK1 ($P<0.05$), VEGFR2 ($P<0.05$) and CD31 ($P<0.05$) IF, presented as the mean fluorescence intensity. (C) Observation of IF staining for vimentin, fibronectin and E-cadherin on serial paraffin sections of xenograft tumors generated using Hep3B wild-type and CRISPR#73 cells with confocal microscopy. (D) Quantification of vimentin ($P<0.05$), fibronectin ($P<0.01$) and E-cadherin ($P<0.05$) IF, presented as the mean fluorescence intensity.

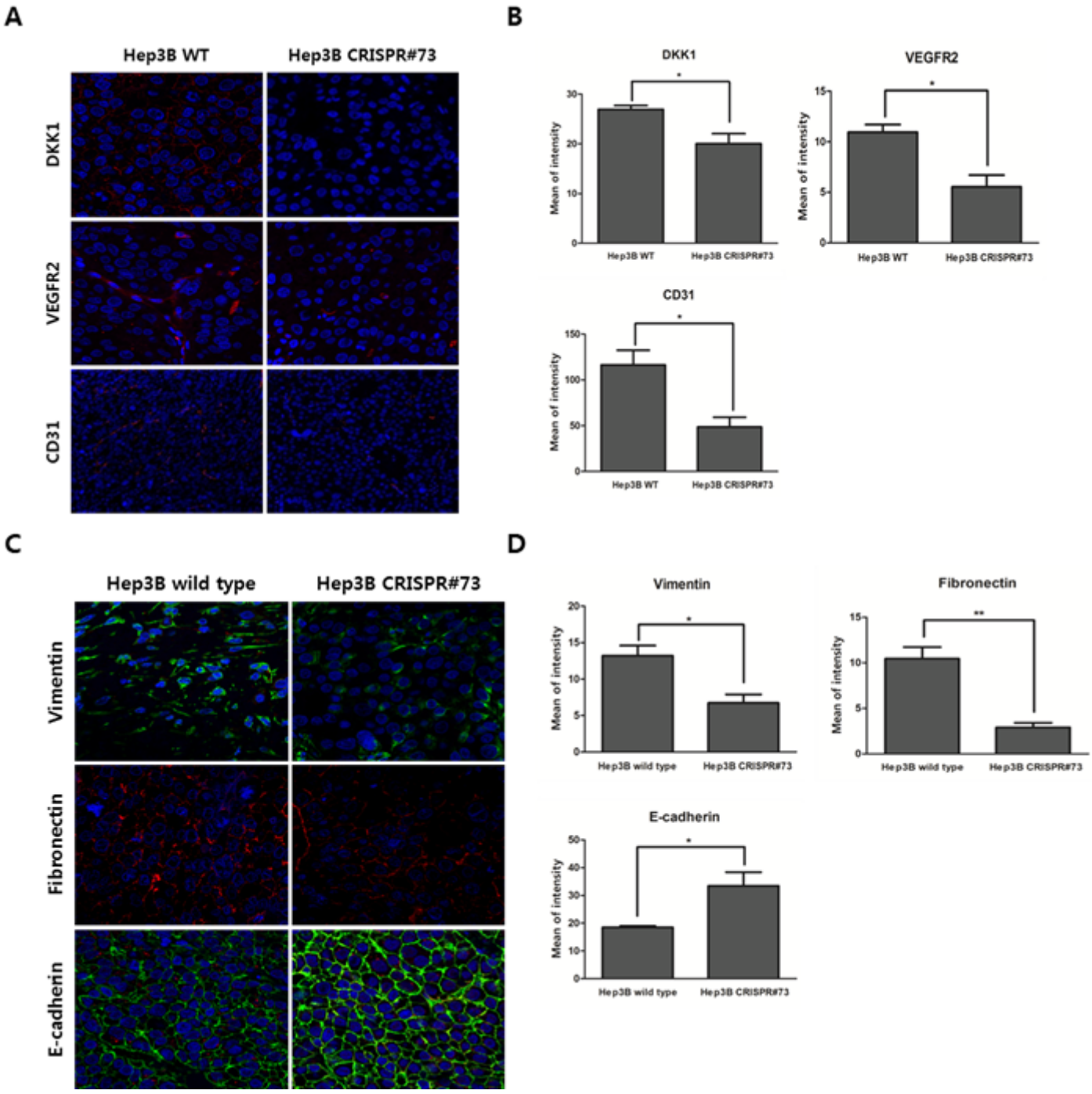

Figure 5

DKK1 increased angiogenesis and metastasis in the xenograft mouse model. (A) Observation of IF staining for DKK1, VEGFR2 and CD31 on serial paraffin sections of xenograft tumors generated using Hep3B wild-type and CRISPR#73 with confocal microscopy. (B) Quantification of DKK1 ($P<0.05$), VEGFR2 ($P<0.05$) and CD31 ($P<0.05$) IF, presented as the mean fluorescence intensity. (C) Observation of IF staining for vimentin, fibronectin and E-cadherin on serial paraffin sections of xenograft tumors generated using Hep3B wild-type and CRISPR#73 cells with confocal microscopy. (D) Quantification of vimentin ($P<0.05$), fibronectin ($P<0.01$) and E-cadherin ($P<0.05$) IF, presented as the mean fluorescence intensity.

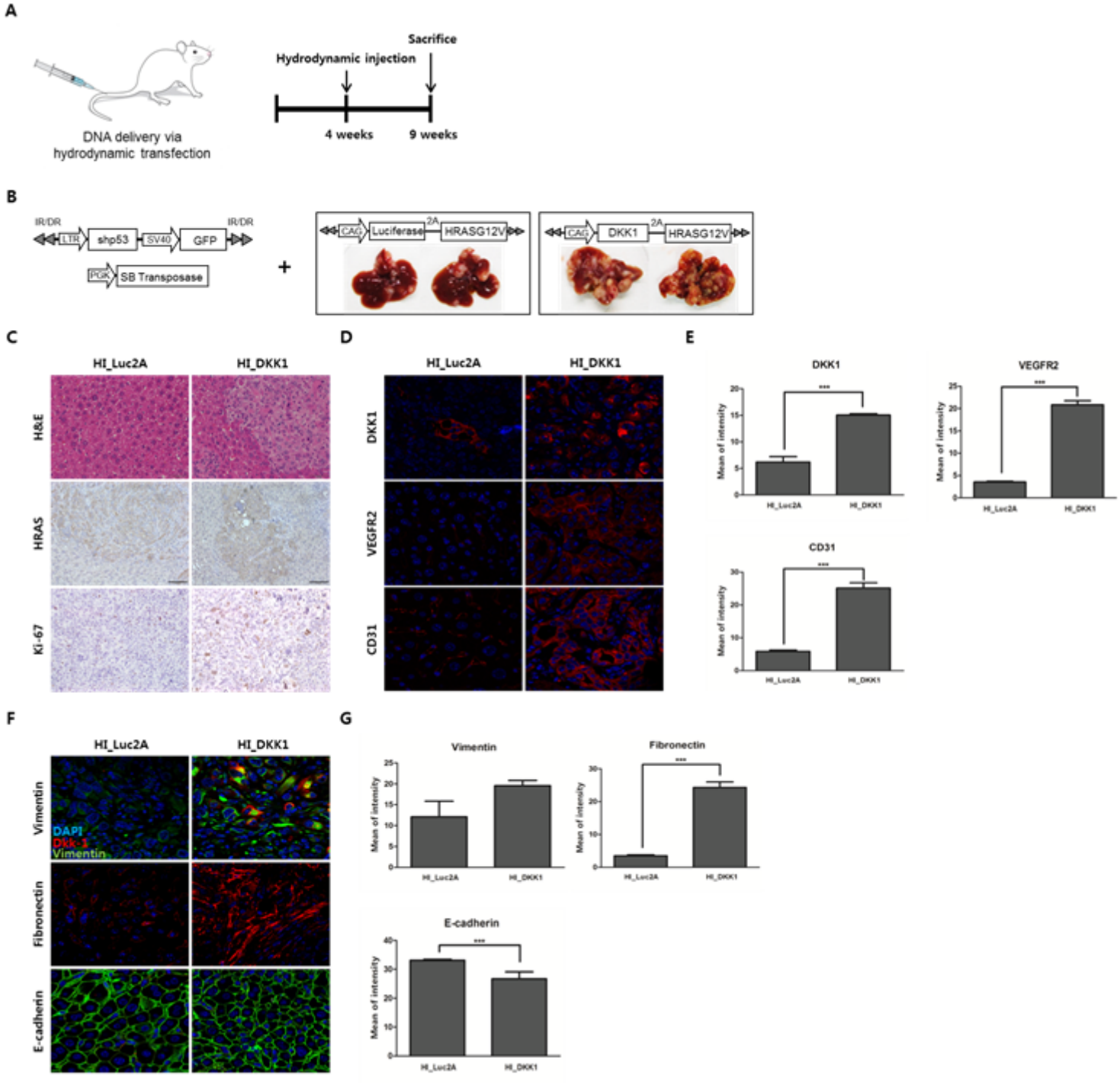

Figure 6

DKK1 increased tumor growth and metastasis in the transgenic mouse model. (A) DNA mixtures were injected into the lateral tail veins of 4-week-old mice and the livers were harvested at 9 weeks. (B) Forced expression of DKK1 with HRAS in transgenic mouse liver resulted in the formation of more tumors (n=5), compared to the controls. (C) H&E and IHC staining for HRAS and Ki-67 on serial paraffin sections of HI_Luc2A and HI_DKK1 tumors. (D) Observation of IF staining for DKK1, VEGFR2 and CD31 on serial paraffin sections of HI_Luc2A and HI_DKK1 tumors using confocal microscopy. (E) Quantification of DKK1, VEGFR2 and CD31 (all P<0.001) IF, presented as the mean fluorescence intensity. (F) IF staining for

vimentin, fibronectin and E-cadherin on serial paraffin sections of HI_Luc2A and HI_DKK1 tumors. (G) Quantification of vimentin, fibronectin (P<0.001) and E-cadherin (P<0.001) IF, presented as the mean fluorescence intensity.

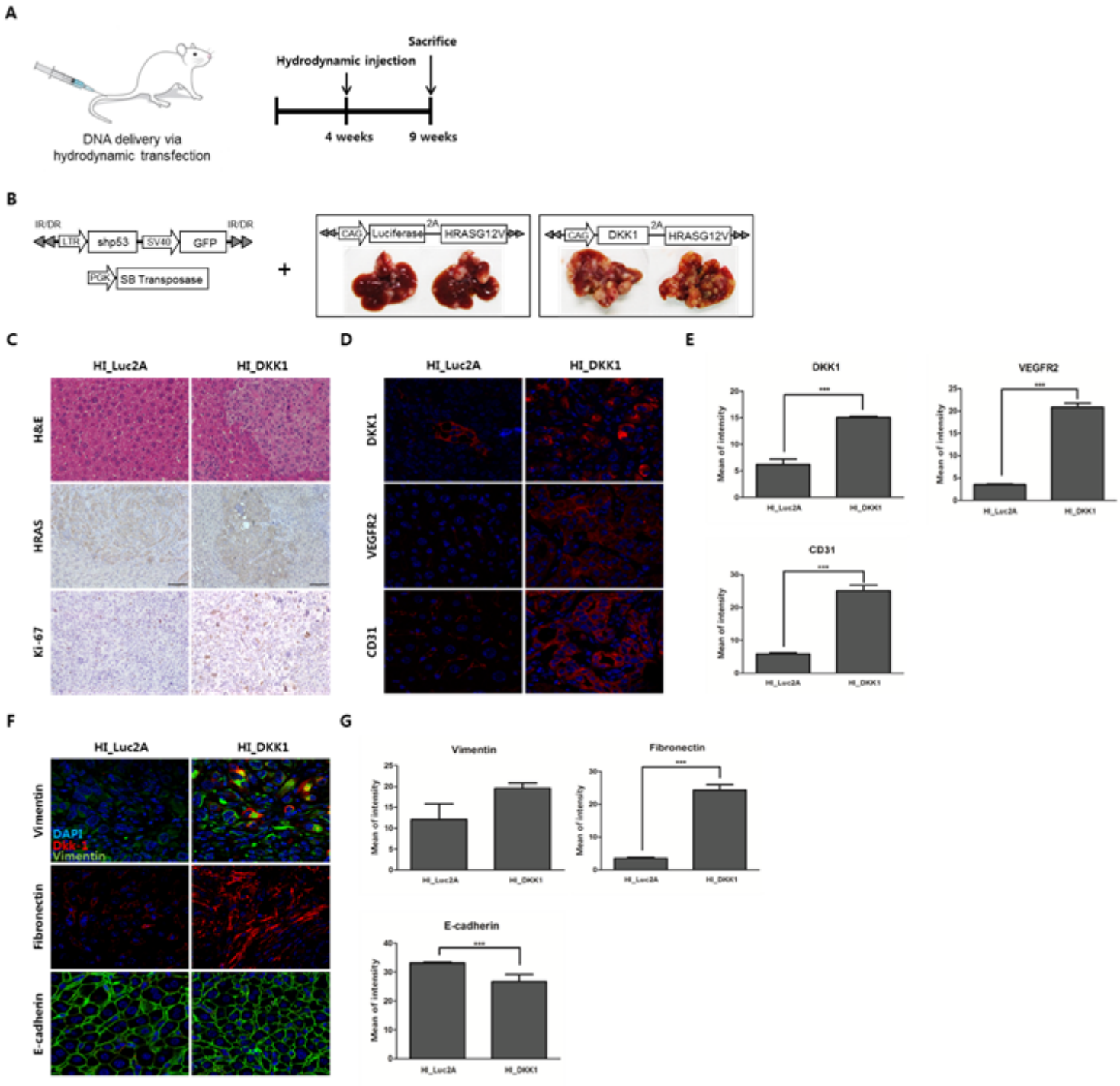

Figure 6

DKK1 increased tumor growth and metastasis in the transgenic mouse model. (A) DNA mixtures were injected into the lateral tail veins of 4-week-old mice and the livers were harvested at 9 weeks. (B) Forced expression of DKK1 with HRAS in transgenic mouse liver resulted in the formation of more tumors (n=5), compared to the controls. (C) H&E and IHC staining for HRAS and Ki-67 on serial paraffin sections of

HI_Luc2A and HI_DKK1 tumors. (D) Observation of IF staining for DKK1, VEGFR2 and CD31 on serial paraffin sections of HI_Luc2A and HI_DKK1 tumors using confocal microscopy. (E) Quantification of DKK1, VEGFR2 and CD31 (all P<0.001) IF, presented as the mean fluorescence intensity. (F) IF staining for vimentin, fibronectin and E-cadherin on serial paraffin sections of HI_Luc2A and HI_DKK1 tumors. (G) Quantification of vimentin, fibronectin (P<0.001) and E-cadherin (P<0.001) IF, presented as the mean fluorescence intensity.

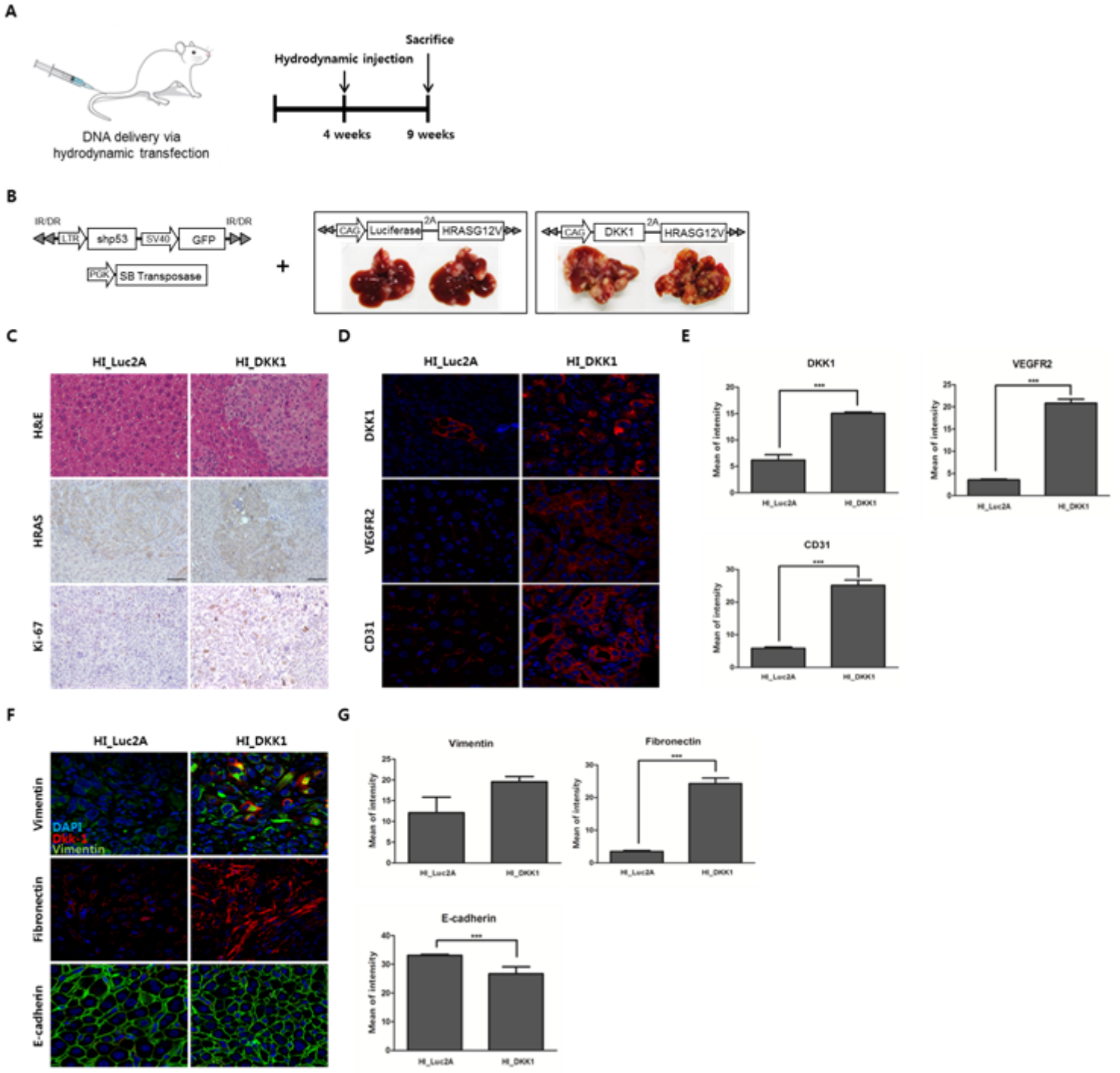

Figure 6

DKK1 increased tumor growth and metastasis in the transgenic mouse model. (A) DNA mixtures were injected into the lateral tail veins of 4-week-old mice and the livers were harvested at 9 weeks. (B) Forced expression of DKK1 with HRAS in transgenic mouse liver resulted in the formation of more tumors (n=5), compared to the controls. (C) H&E and IHC staining for HRAS and Ki-67 on serial paraffin sections of HI_Luc2A and HI_DKK1 tumors. (D) Observation of IF staining for DKK1, VEGFR2 and CD31 on serial paraffin sections of HI_Luc2A and HI_DKK1 tumors using confocal microscopy. (E) Quantification of DKK1, VEGFR2 and CD31 (all $P<0.001$) IF, presented as the mean fluorescence intensity. (F) IF staining for vimentin, fibronectin and E-cadherin on serial paraffin sections of HI_Luc2A and HI_DKK1 tumors. (G) Quantification of vimentin, fibronectin ($P<0.001$) and E-cadherin ($P<0.001$) IF, presented as the mean fluorescence intensity.

Supplementary Files

This is a list of supplementary files associated with this preprint. Click to download.

- figS1.png
- figS1.png
- figS1.png
- figS2.png
- figS2.png
- figS2.png
- figS3.png
- figS3.png
- figS3.png